

Environmental Science Processes & Impacts

Accepted Manuscript



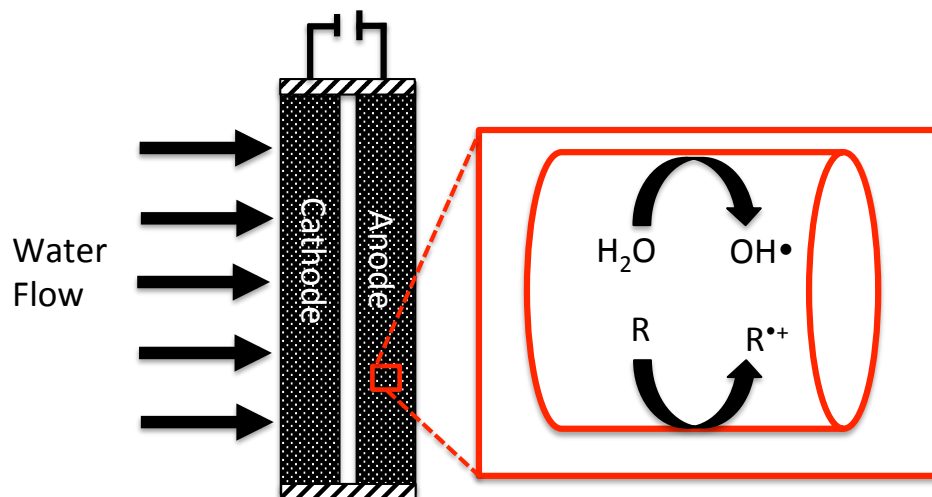
This is an *Accepted Manuscript*, which has been through the Royal Society of Chemistry peer review process and has been accepted for publication.

Accepted Manuscripts are published online shortly after acceptance, before technical editing, formatting and proof reading. Using this free service, authors can make their results available to the community, in citable form, before we publish the edited article. We will replace this *Accepted Manuscript* with the edited and formatted *Advance Article* as soon as it is available.

You can find more information about *Accepted Manuscripts* in the [Information for Authors](#).

Please note that technical editing may introduce minor changes to the text and/or graphics, which may alter content. The journal's standard [Terms & Conditions](#) and the [Ethical guidelines](#) still apply. In no event shall the Royal Society of Chemistry be held responsible for any errors or omissions in this *Accepted Manuscript* or any consequences arising from the use of any information it contains.

A critical review of the literature focused on electrochemical advanced oxidation processes for water treatment



Environmental Impact Statement

Pollution by recalcitrant organic compounds is a significant environmental problem. To prevent the release of these compounds, new advanced treatment methods must be developed that can operate efficiently and sustainably. This paper provides a critical review of electrochemical advanced oxidation processes (EAOPs). This novel technology has promise for treating a wide variety of recalcitrant contaminants. The review focuses on unifying the state of knowledge related to EAOPs in order to provide an understanding of their operation and the environmental impacts that result in their use. Key challenges of the technology are presented and future research directions are discussed.

Critical Review of Electrochemical Advanced Oxidation Processes for Water Treatment Applications

Cite this: DOI:

10.1039/x0xx00000x

Brian P. Chaplin*

*Department of Chemical Engineering, University of Illinois at Chicago
810 S. Clinton Ave., Chicago, IL 60607, USA. E-mail: chaplin@uic.edu; Tel: +1 (312) 996 0288

Received 00th January 2012,

Accepted 00th January 2012

DOI: 10.1039/x0xx00000x

www.rsc.org/

Electrochemical advanced oxidation processes (EAOPs) have emerged as novel water treatment technologies for the elimination of a broad-range of organic contaminants. Considerable validation of this technology has been performed at both the bench-scale and pilot-scale, which has been facilitated by the development of stable electrode materials that efficiently generate high yields of hydroxyl radicals (OH•) (e.g., boron-doped diamond (BDD), doped-SnO₂, PbO₂, and substoichiometric- and doped-TiO₂). Although a promising new technology, the mechanisms involved in the oxidation of organic compounds during EAOPs and the corresponding environmental impacts of their use have not been fully addressed. In order to unify the state of knowledge, identify research gaps, and stimulate new research in these areas, this review critically analyses published research pertaining to EAOPs. Specific topics covered in this review include 1) EAOP electrode types, 2) oxidation pathways of select classes of contaminants, 3) rate limitations in applied settings, and 4) long-term sustainability. Key challenges facing EAOP technologies are related to toxic byproduct formation (e.g., ClO₄⁻ and halogenated organic compounds) and low electro-active surface areas. These challenges must be addressed in future research in order for EAOPs to realize their full potential for water treatment.

I. Introduction

Electrochemical advanced oxidation processes (EAOPs) have emerged as promising technologies for the destruction of recalcitrant and complex waste streams. Hydroxyl radicals (OH•) are formed via the oxidation of water on the anode surface, as shown in equation 1.



These OH• react unselectively with a wide range of recalcitrant organics, often at diffusion-limited rates.¹ Various electrodes have been applied to EAOPs and the most common materials include doped-SnO₂,^{2,5} PbO₂ and doped-PbO₂,^{6,11} boron-doped diamond (BDD),^{12,16} and substoichiometric- and doped-TiO₂.¹⁷⁻²⁰ A common feature of these electrodes is that a high overpotential is necessary to facilitate electrochemical O₂ production, which allows reaction (1) to take place prior to O atom paring and O₂ evolution. Additionally, it is thought that OH• have a very weak interaction with the electrode surface, which allows them to be available for substrate oxidation at and near the anode surface.²¹⁻²⁷ Since water is not oxidized on EAOP electrodes until ~ 2.0 V versus the standard hydrogen electrode (SHE), there is a large electrode potential window available for direct electron transfer (DET) reactions. It has been shown that DET reactions constitute an additional mechanism for

compound oxidation, where an electron is transferred directly from the contaminant (R) to the anode (equation (2)).



The importance of the DET pathway is often overlooked, and it has been shown to be a critical rate-limiting step for the oxidation of recalcitrant compounds that are unreactive towards OH• (e.g., fluorinated organics).^{5,16} Various other studies have shown that a combination of DET reactions and reaction with OH• are involved in the oxidation pathways of a number of organic compounds.^{14,17,28,29} A large number of studies have shown that EAOPs are effective at the mineralization of numerous recalcitrant compounds, including but not limited to phenolic compounds,^{2,3,7,8,12,14,15,20,24,30-38} perfluorinated organics,^{5,16,39-42} chlorinated organics,⁴³ disinfection byproducts,^{28,29} bulk organics in reverse osmosis concentrates,^{29,44-48} and landfill leachates,⁴⁹⁻⁵⁷ pharmaceuticals,⁵⁸⁻⁶¹ endocrine disruptors,^{62,63} human waste,⁶⁴ and various industrial waste streams.⁶⁵⁻⁷⁴

Traditional advanced oxidation processes (AOPs) that produce OH• by the activation of H₂O₂ via the Fenton process, UV light or ozone have emerged as effective water treatment technologies.⁷⁵⁻⁷⁸ Although AOPs suffer from high capital and operating costs and decreased efficiency in natural waters due to OH• scavenging,^{75,79,80} they are more frequently being used due to the ability of OH• to destroy contaminants that are resistant to conventional treatment

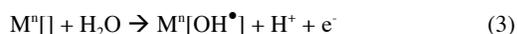
technologies.⁸¹⁻⁸³ Although not a direct replacement for AOPs, EAOPs have several advantages. Chemical addition is not needed for EAOPs as OH^\bullet are generated directly from water oxidation (equation 1). Contaminants that are unreactive with OH^\bullet can be degraded by EAOPs via DET reactions (e.g., fluorinated organics).^{5,16} Studies have shown that an acidic boundary layer is produced at the anode surface due to water oxidation (see equation 1), in this region HCO_3^- is protonated to H_2CO_3 and therefore prevents OH^\bullet scavenging associated with HCO_3^- present in natural waters.²⁹ Studies have also shown that there is an opportunity for energy recovery from EAOPs by capturing the H_2 that is produced from cathodic reactions during simultaneous oxidation of organic compounds on the anode.⁸⁴ Studies have also shown that the operation of EAOPs is cheaper than traditional AOPs under certain operating conditions.^{29,80,85}

This review focuses on published research in the area of EAOPs. I summarize the state of knowledge pertaining to 1) electrode types, 2) reaction pathways of important classes of contaminants, 3) rate limitations in applied settings, and 4) long-term sustainability. Future research needs are discussed in the context of addressing gaps in the state of knowledge and limitations associated with EAOPs. A specific focus of this review is related to the physical and chemical processes involved in compound oxidation during EAOPs, and the corresponding environmental impacts of this treatment method. Specific environmental impacts addressed include toxic byproduct formation and the assessment of EAOPs from a life cycle perspective. Of the electrode materials reviewed, a specific focus is dedicated to BDD electrodes, as they are the most promising and therefore most researched EAOP electrode. This review only considers processes involving the formation of OH^\bullet via water oxidation at an anode surface and does not consider the formation of OH^\bullet from electro-Fenton, photoelectrochemical, sonoelectrochemical, and other chemical/electrochemical methods. Excellent review articles exist on these various topics.^{75-78,86-92} Several review articles have also been published related to electrochemical oxidation for water treatment.⁹³⁻⁹⁹ This review seeks to add to the existing body of knowledge by concisely summarizing the important pathways of contaminant transformation and byproduct formation at EAOP electrodes, with a focus on interpreting both experimental and density functional theory (DFT) studies in order to understand key advantages and disadvantages of EAOPs and prioritize future research that will facilitate widespread adoption of EAOPs for water treatment.

II. State of Knowledge

A. Electrode Types

EAOP electrodes are classified as inactive electrodes, which are electrode materials whose atoms do not change oxidation state during electrochemical reactions. An example of this process is shown in equation (3):

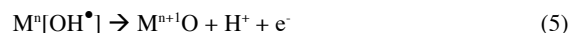


where $\text{M}^n[]$ is an electrode surface site in an oxidation state n , and $\text{M}^n[\text{OH}^\bullet]$ is a OH^\bullet that is physically adsorbed at a surface site.²¹ Oxygen evolution on inactive electrodes is thought to occur through the reaction between an additional H_2O molecule and $\text{M}^n[\text{OH}^\bullet]$ site to form O_2 , as shown in equation (4).²¹



The exact mechanism of the reaction shown in equation (4) is unknown, but it has been speculated to involve intermediate H_2O_2 production on BDD electrodes.^{13,25} The weak interaction of OH^\bullet

with inactive electrodes requires a high anodic potential for water oxidation (~ 2.0 V/SHE).^{97,100} By contrast, active electrodes (e.g., Pt, IrO_2) continually cycle oxidation states during electrochemical oxidation of substrates. The $\text{M}^n[\text{OH}^\bullet]$ sites on active electrode materials are further oxidized to a higher M^{n+1} oxide, as shown in equation (5).



The formation of OH^\bullet on active anodes is low, and the oxidation of substrates (R) primarily occurs via an oxygen transfer reaction, which restores the surface site to its original oxidation state (M^n), as shown in equation (6).



Support for the above mechanism on inactive electrodes was obtained by the detection of ^{18}O within an IrO_2/Ti electrode from ^{18}O -enriched water.¹⁰¹ The subsequent oxidation of formic acid resulted in the transfer of ^{18}O into the CO_2 oxidation product.¹⁰¹ The relative life time of O atoms on active electrodes are increased due to adsorption at the electrode surface, allowing O atom pairing to occur via surface diffusion and thus active electrodes are characterized with a lower potential for oxygen evolution (~ 1.5 V/SHE) relative to inactive electrodes. Additionally, since OH^\bullet are not generated in sufficient quantities, active anodes often promote only partial oxidation of substrates.^{21,102-104}

The high production of OH^\bullet at inactive anodes facilitates the EAOP technology for compound oxidation in aqueous systems. The most effective inactive electrodes for EAOPs are doped- SnO_2 , PbO_2 , BDD, and sub-stoichiometric and doped- TiO_2 . The classification of these electrodes as inactive anodes is based primarily on their ability to form high yields of OH^\bullet . However, as will be shown in the discussion below, not all electrodes cleanly divide into the active and inactive classification, and some electrodes have characteristics of both anode types.

A.1. Doped- SnO_2 Electrodes. The conductivity of SnO_2 is low, and thus it must be doped to obtain high conductivity and allow it to function as an effective EAOP electrode. The most common dopant is Sb, which has resulted in an electrode with high conductivity and a potential for O_2 evolution of ~ 1.9 V/SHE.⁹⁷ However, Sb is a toxic substance with an EPA drinking water limit of $6 \mu\text{g L}^{-1}$.¹⁰⁵ Therefore, research has focused on the use of other dopants (e.g., Ar, B, Bi, F, Cl, P).¹⁰⁶⁻¹⁰⁹ The formation of OH^\bullet at SnO_2 electrodes has been concluded based on spin trap experiments²¹ and the mineralization of aqueous substrates.^{2,21,110} While many studies have investigated the use of doped- SnO_2 electrodes in laboratory settings,^{3-5,33,111-118} they are not commercially available due to a short service life.^{119,120} Two mechanisms for deactivation of these electrodes have been proposed. The first mechanism is attributed to the formation of a nonconductive Sn hydroxide layer on the outer surface of the anode,^{108,121,122} and the second is due to passivation of the underlying Ti substrate that causes doped- SnO_2 film delamination.^{108,122} The Sn hydroxide surface layer was proposed to form due to hydration of the SnO_2 surface,^{108,122} and can be largely mitigated by doping with Pt.^{122,123} Passivation of the Ti support can be minimized by the placement of an IrO_2 interlayer between the Ti substrate and SnO_2 - Sb_2O_5 coating, which has resulted in a significant improvement in service life.^{115,120} The IrO_2 interlayer is stable under high anodic polarization and Ir atoms are able to undergo isomorphic substitution with both Ti and Sn atoms at the two metal-metal interfaces.^{115,120} Therefore, the electrodes are more resistant to delamination at the Ti substrate and the interface between IrO_2 and SnO_2 layers. Other coatings, for example F-doped

SnO₂, have also resulted in improved electrode longevity.¹²⁴

Although various studies on the oxidation of organic compounds at doped-SnO₂ electrodes exist, little work has been conducted on understanding the mechanisms of compound transformation at these electrodes.⁵ Unifying the interactions of doped-SnO₂ electrodes with aqueous substrates from a review of the literature is difficult due to the various dopant quantities and types used in various studies. It has been suggested that compound adsorption is involved in the oxidation mechanisms of organic compounds at doped-SnO₂ electrodes.^{24,125} These results suggest that doped-SnO₂ electrodes may have a catalytic effect on DET reactions of aqueous substrates, but further research focused on elucidating mechanisms of compound oxidation at these electrodes are needed.

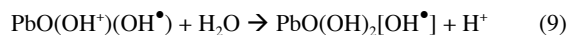
A.2. PbO₂ Electrodes. Early studies of compound oxidation at PbO₂ electrodes utilized packed-bed reactors containing oxidized Pb pellets.^{6,126} Later studies explored PbO₂ and doped-PbO₂ anodes on a variety of substrates (e.g., Ta, Ti, stainless steel, Ebonex®).^{11,127-135} The generation of OH[•] on PbO₂ electrodes has been confirmed in several studies.^{11,136-138} However, the mechanism for OH[•] generation at the PbO₂ electrode is still not well understood. Research focused on PbO₂ electrodes for lead acid batteries, postulated that OH[•] formation occurs in a hydrated Pb oxide gel layer, that forms on the outer electrode surface.^{22,139} This mechanism assumes an equilibrium between the bulk PbO₂ crystal phase and the hydrated lead oxide gel layer (PbO(OH)₂). The gel layer forms linear polymer chains that are both electrically and proton conductive. The equilibrium between these zones is shown in equation (7).



Upon anodic polarization of the anode, electron conduction through the gel layer is postulated to occur via a hopping mechanism from one Pb⁴⁺ ion to the next.¹³⁹ Therefore, the active centers within the gel layer become oxidized, as shown in equation (8).



A subsequent reaction with water neutralizes the positive charge on the active site, and generates a physically adsorbed OH[•] ([OH[•]]), as shown in equation (9).



These weakly adsorbed OH[•] are available for substrate oxidation, and various studies have shown that the oxidation efficiency of organic compounds at PbO₂ electrodes is close to that of BDD electrodes.³⁰

Various dopants (e.g., Fe, Co, Bi, F) have been added to PbO₂ electrodes, and their main influence on electrochemical performance was reducing the crystal grain size, which correlated to higher electrochemical activity due to a higher electroactive surface area.¹⁴⁰ It also has been shown that the β-PbO₂ crystal structure is more porous than the α-PbO₂ crystal structure and thus the former shows higher oxidation rates.¹⁴¹ Recent studies have shown that doping PbO₂ electrodes with a fluorine resin resulted in higher OH[•] production and a higher overpotential for oxygen evolution (~ 2.5 V/SHE for doped-PbO₂ versus 1.9 V/SHE for PbO₂).¹¹ The change in electrochemical performance upon doping was attributed to the hydrophobic surface, but the mechanism was not investigated. It is likely that the weaker interaction of OH[•] with the hydrophobic surface allowed them to be more available for compound oxidation. The results may also be influenced by the hydrophobicity of the contaminant chosen to evaluate the performance of the electrodes,

which was the hydrophobic pesticide 2,4-dichlorophenoxyacetic acid (Log K_{ow} = 2.81).¹¹

The slow leaching of Pb ions into solution is a concern for water treatment applications, which has limited the appeal of PbO₂ anodes. However, experiments have shown that PbO₂ electrodes are stable during anodic polarization, and Pb leaching is minimal.¹⁴² Nevertheless, due to the toxicity of Pb and the environmental regulations set forth by the EPA (15 µg L⁻¹ drinking water standard) and other regulatory agencies, the use of PbO₂ electrodes for water treatment applications should be approached with caution.

A.3. Doped- and Sub-stoichiometric TiO₂. The conductive Magneli phase suboxides of TiO₂, and doped-TiO₂ are very promising electrode materials for water treatment. Stoichiometric titanium dioxide (TiO₂) is an insulator with an electrical conductivity of ~10⁻⁹ Ω⁻¹ cm⁻¹.¹⁴³ The electronic properties of TiO₂ can be drastically changed by creating oxygen deficiencies in the lattice structure, which is accomplished at temperatures above 900 °C and under a H₂ atmosphere or in the presence of reduced metals (e.g., Ti), or by incorporation of group five elements such as V, Nb, or Ta. Both methods result in conversion of some Ti^(IV) to Ti^(III) and n-type semiconductor behavior.

There are several suboxides of TiO₂, collectively known as Magneli phases (Ti_nO_{2n-1}, 4 ≤ n ≤ 10), where the most conductive compounds of the series are Ti₄O₇ and Ti₅O₉, and thus are the desired components during synthesis. For example, Ti₄O₇ has an electrical conductivity of 166 Ω⁻¹cm⁻¹, many orders of magnitude greater than TiO₂.¹⁴³ The oxygen-deficiency of Magneli phases are due to edge sharing of TiO₆ octahedra in the crystallographic shear planes.¹⁴⁴ Over-reduction of TiO₂ creates a structure with significant oxygen deficiencies, which is extremely brittle and less conductive than Ti₄O₇.¹⁴³ Reduction methods have been tailored to synthesize materials consisting primarily of Ti₄O₇, as confirmed by XRD measurements.^{143,145} Ceramic Magneli phase electrodes consisting primarily of Ti₄O₇ are commercially available, and are known by the trade name Ebonex®.¹⁴³ Ebonex has been used in various lab-scale water treatment applications,^{18-20,64,146,147} and recent work comparing Ebonex® electrodes to BDD concluded that the OH[•] produced on Ebonex® are less abundant but more reactive than those formed on BDD.¹⁹ The primary application of Ti₄O₇ electrodes are the cathodic protection of metal structures.¹⁴⁸ However, due to its corrosion resistance and electrochemical stability there is growing interest in the synthesis and testing of Ti₄O₇ electrodes as supports for batteries, fuel cells, catalysts, and electrocatalysts.^{145,146,148-152}

Due to the oxygen deficient nature of substoichiometric TiO₂, there is a possibility for oxygen incorporation into the lattice structure during anodic polarization and thus the formation of a passivating TiO₂ coating.^{144,153} Studies have shown through conductivity and electrochemical impedance spectroscopy (EIS) measurements that passivation can occur under mild electrochemical polarization (e.g., ~ 1.6 V/SHE).^{144,153} However, some studies have reported that the passivation was reversible upon cathodic polarization,¹⁵⁴ while other studies have found that the passivation was irreversible.¹⁴⁴ The discrepancies in results are not clear and may be due to the presence of different Magneli phases in the samples tested. Recent work with Ti₄O₇ (Ebonex) electrodes has shown that periodic polarity reversals during the oxidation of sulfide were able to prevent electrode passivation.¹⁵⁴ These studies indicate that Ti₄O₇ exhibits properties attributed to both inactive and active anodes. That is, inactive anodes characteristically form OH[•] during water oxidation, and active anodes form a higher oxide during water oxidation. However, the higher oxide that is formed (TiO₂) is unable

to participate in oxygen transfer reactions and thus substrate oxidation.¹⁵⁴ More detailed studies of the passivation of Ti_4O_7 and re-reduction of the proposed TiO_2 passivation layer are needed. Since TiO_2 is only reduced to Ti_4O_7 at elevated temperatures (e.g., 900 °C),¹⁵⁵ the mechanism of passivation/reactivation needs to be studied more closely.

Doping of TiO_2 (rutile phase) with Nb has also been found to produce ceramic materials with very high electrical conductivities. Niobium-doped rutile (NDR) oxides with the general formula of $Ti_{1-x}Nb_xO_2$ ($0 \leq x \leq 0.8$) have been studied and found to be highly conductive.^{149,156} For example, the oxide with the composition of $Ti_{0.9}Ni_{0.1}O_2$ has an electrical conductivity similar to that of Ti_4O_7 .¹⁴⁹ Doping occurs by direct substitution of Nb^{5+} for Ti^{4+} , which is accomplished due to the similar crystal radii of Nb^{5+} and Ti^{4+} when present in a 6-coordinate structure.¹⁵⁷ Therefore, doped oxides have the advantage of having negligible anion deficiencies,¹⁵⁶ making them much more resistant to oxidation than Ti_4O_7 .¹⁴⁹ In fact, oxidative wear of NDR electrodes has been found to be reversible via polarization of the electrode as a cathode.¹⁴⁹ This unique feature has resulted in using NDR electrodes in unitized regenerative fuel cells.¹⁵³ NDR electrodes have been researched for other electrochemical technologies including fuel cell and battery supports,¹⁵⁸⁻¹⁶⁰ dye-sensitized solar cells,¹⁶¹⁻¹⁶⁴ water splitting,¹⁶⁵ and gas sensors.^{166,167} Doping TiO_2 with other transition metals has also produced stable and conductive electrodes, which have been tested as O_2 evolving electrocatalysts.¹⁶⁸ Surprisingly, only one study could be found that used doped- TiO_2 for EAOPs,¹⁷ but the durability and electrochemical stability of this electrode warrants more investigation.

The water treatment potential of both Ti_4O_7 and NDR electrodes are very promising, although few studies on these materials exist. Both electrode materials can produce $OH\cdot$ via water oxidation,^{17,19,20,150} Recent work has also taken advantage of the porous monolithic structure of Ti_4O_7 electrodes to utilize them as a reactive electrochemical membrane.²⁰ Future research should focus on understanding these electrodes from a more fundamental perspective, as few studies have attempted to study the mechanisms of charge transfer at the surface of substoichiometric- and doped- TiO_2 anodes.

A.4. Boron-doped Diamond Electrodes. The most promising and widely studied electrode for EAOPs is BDD. BDD electrodes are commonly produced by the chemical vapor deposition (CVD) method. The CVD method is relatively inexpensive and has resulted in a widespread interest in polycrystalline diamond films for industrial applications.⁹⁶ Boron is the most common dopant used in diamond electrodes due to its low charge carrier activation energy (0.37 eV).¹⁶⁹ The boron atoms substitute for carbon atoms in the diamond lattice giving a p-type semiconductor, where the dopant consumes an extra electron for chemical bonding thus creating excess holes in the semiconductor.¹⁷⁰ At low doping levels ($\sim 10^{17}$ atoms cm^{-3}), the diamond exhibits semiconductor properties with conduction occurring by a hole hopping mechanism.¹⁷¹ At high doping levels ($\sim 10^{20}$ atoms cm^{-3}), the diamond exhibits semi-metallic conductivity, due to impurity bands of low energy that allows electron conduction, where metallic resistivities $< 0.1 \Omega\text{-cm}$ are commonly achieved.¹⁷² BDD electrodes have been synthesized as microcrystalline¹⁷³⁻¹⁷⁵ and nanocrystalline¹⁷⁶⁻¹⁸¹ materials. The electrochemical response of redox active species in solution has been shown to differ as a function of crystal size and synthesis method.¹⁸² The smaller crystal size translates to a larger proportion of grain boundaries, which leads to a higher content of sp^2 C at the grain boundaries,¹⁷⁸ and also may lead to enhanced corrosion rates via

oxidation of edge sites to CO_2 at high currents.¹⁸¹ However, more studies are needed to determine if significant differences in oxidation rates of organics and prevailing reaction mechanisms occur as a function of crystal size, as these studies are currently lacking.

BDD electrodes are known for their extreme stability under anodic polarization, which is due to the C atoms being in sp^3 hybridization. However, BDD film electrodes are still subject to failure, primarily due to film delamination from the substrate,¹⁸⁰ and wear at grain boundaries is also possible at high applied current densities (e.g., 1 A cm^{-2}).¹⁸¹ The traditional substrate for diamond electrodes is p-silicon, because it is able to form a compact self-limiting oxide and has a relatively low electrochemical activity, which prevents film delamination.¹⁸⁰ However due to the fragility of Si, which makes it non-ideal for industrial applications, various studies have investigated different substrates for the BDD films, including Ta, Nb, W, Zr, C, Ti, and various interlayers on metal substrates.^{180,183-187} One study found that the approximate substrate stability of nanocrystalline BDD electrodes followed the order of: Ta > Si > Nb > W \gg Ti.¹⁸⁰ The most important factor to prevent film delamination is matching the CTE value for diamond (CTE = $1.18 \times 10^{-6} K^{-1}$)¹⁸⁸ and that of the substrate. A large difference between the CTE value of diamond and the substrate can lead to defects in the film that allow electrolyte permeation through the BDD film and cause corrosion of the substrate. It has been found that the most resistant substrates to film delamination are metals whose CTE values decrease from the metal substrate to its corresponding oxide.¹⁸⁰ For such metals the oxide is more compact than the pure metal and thus will not result in delamination of the BDD film when the substrate becomes oxidized. This scenario is the case for Si and Ta, and both have been shown to be very stable electrode substrates.¹⁸⁰ A CTE increase from the metal to the oxide results in a physical expansion of the oxide that promotes BDD delamination. This scenario was the case for Nb, W, and Ti, which resulted in BDD film delamination.¹⁸⁰ An additional method to improve film adhesion was roughening the substrate (e.g., bead blasting), which increased the density of nucleation sites for the BDD film and therefore reduced the overall film stress.^{180,189} Various strategies have been employed to improve the adhesion of BDD films to a Ti substrate and overcome the ~ 10 -fold difference in CTE value compared to diamond. The use of Ti is desirable because it is inexpensive, highly conductive, and much more robust than Si. Various studies have utilized interlayers between Ti and the BDD film that include Si,¹⁸⁷ Ta,¹⁸⁴ and nanocrystalline BDD.¹⁹⁰ Increasing the stability of BDD/Ti electrodes is an on going area of research, with the ultimate goal of decreasing the cost of BDD electrodes.

Past research showed that the boron dopant concentrates at grain boundaries, crystal edges, and other defects.¹⁹¹ This information has led many to believe that the electrochemical activity of BDD electrodes is primarily concentrated at these sites. However, careful characterization of a hydrogen-terminated BDD surface using conductive probe atomic force microscopy (CP-AFM) and scanning electrochemical microscopy (SECM) showed that the majority of the electrode was nonconductive and only discrete random areas showed high conductivity.¹⁹² The electrochemical active surface area was strongly correlated with the boron-doping level.¹⁹² More recent work using a more sensitive scanning electrochemical cell microscopy (SECCM) technique showed that the entire BDD surface was electroactive.¹⁹³ However, the electrochemical activity towards multiple redox couples was shown to vary between different crystal facets, and was also linked to boron-doping levels.¹⁹³ Evidence was not found for increased activity at grain boundaries,¹⁹³ as previously believed.

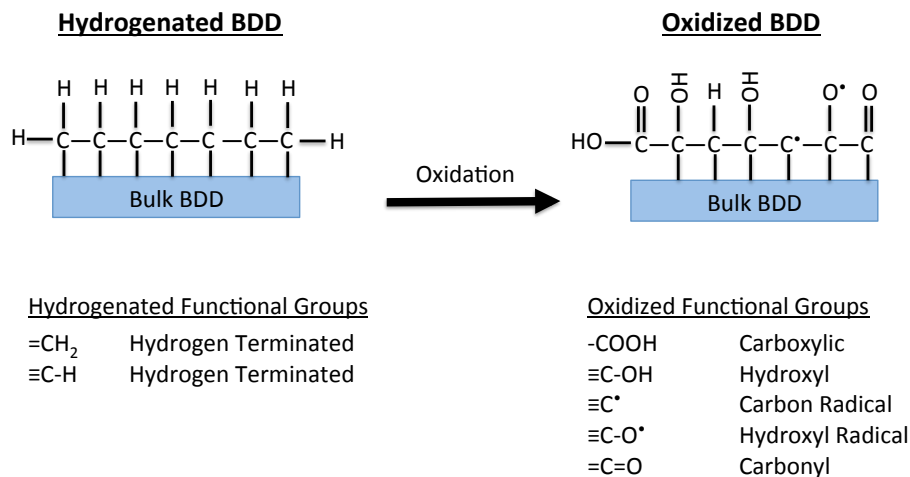


Figure 1. Prevalent functional groups present on the hydrogenated and oxidized BDD surface.

The surface functional groups of BDD electrodes have been shown to have a significant effect on charge transfer at the electrode surface. As shown in Figure 1, freshly prepared electrodes are H-terminated (i.e., =CH₂, ≡C-H), but anodic polarization creates various oxygenated-functional groups (i.e., hydroxyl (≡C-OH), carbonyl (=C=O), carboxyl (-COOH)) that have been detected by X-ray photoelectron spectroscopy (XPS) measurements.^{172,180,181,194-198} The ≡C-OH groups form along the crystal planes and -C-OOH and =C=O groups form at defect and edge sites. As a result, the density of specific functional groups are a function of the crystal size, which are consistent with XPS measurements that showed a much higher density of =C=O sites on nanocrystalline BDD electrodes,^{180,181} compared to microcrystalline BDD electrodes.¹⁹⁹ A recent study has detailed the formation of these various oxygenated functional groups using density functional theory (DFT) calculations.¹⁸¹ It is suggested that these oxygenated functional groups are subject to further oxidation, that results in the formation of carbon radical (≡C•) and deprotonated hydroxyl radical sites (≡C-O•), as shown in equations (10) and (11).^{181,200}



These radical sites are hypothesized to be active for compound oxidation.^{181,200} Various other studies have shown that the functional groups on the BDD surface have a strong effect on charge transfer during both anodic and cathodic reactions.^{196,200-203} The formation of oxygenated groups from anodic polarization inhibit some reactions while facilitating other types of reactions.²⁰⁰⁻²⁰³ The effect of surface functional groups on DET reaction rates of aqueous compounds have been reported to be attributed to hydrophobic, dipole, and catalytic interactions.^{179,181,201} However, it is often difficult to distinguish between these various effects, and the dominant effect may change as a function of the applied potential. For example, it is hypothesized that dipole-dipole interactions greatly affect the charge transfer of the Fe(CN)₆^{4-/3-} redox couple at the oxygenated BDD electrode surface.²⁰¹ This effect is likely considerable at the redox potential of the Fe(CN)₆^{4-/3-} redox couple (E° = 0.436 V/SHE at pH 7). However, at higher potentials the anode surface is positively polarized, and it thus is unlikely that the surface oxygen groups are negatively charged, and therefore dipole-dipole interactions would not be significant. Therefore, it is important to characterize the effect of functional groups on target

compounds at electrode potentials of interest in order to better understand their effect on charge transfer and prevailing reaction mechanisms. These types of studies are often difficult due to interference from O₂ and OH• production at high electrode potentials. Therefore, fundamental research to understand the affect of BDD functional groups on compound transformation would be greatly aided by experimental studies complemented by DFT calculations.

The mechanism for OH• production on BDD electrodes has been a topic of interest to researchers, and has been shown to be linked to the functional groups present at the electrode surface.¹⁸¹ Experimental results indicate that the over-potential for water oxidation decreases upon oxidation of the BDD surface,¹⁸¹ indicating that the incorporation of oxygen atoms into the BDD surface may catalyze water oxidation. DFT calculations confirmed experimental findings showing that the electrode potential necessary for the activationless oxidation of water to form OH• decreased from 2.74 V/SHE to 2.29 V/SHE when adding oxygenated functional groups (=C=O and ≡C-O• sites) to DFT simulations.¹⁸¹ These results indicate that the role of functional groups on the anode surface should be investigated in more detail, as the BDD surface has long been considered inert and lacking adsorption sites.

B. Oxidation Pathways

Several different chemical classes of substrates have been oxidized at EAOP electrodes. Because the specific reaction pathways differ between and within specific chemical classes, due to the diverse array of compounds oxidized at EAOP electrodes, a complete review of the literature would be impractical. Instead select important chemical classes of substrates are reviewed, with specific focus on environmentally relevant compounds with differing molecular properties (e.g., hydrophobicity, prevailing oxidation mechanism, and chemical structure). For these reasons, the oxidation of phenols, aliphatic acids, and perfluorinated organic compounds were chosen for further review. The key chemical properties of various compounds within each chemical class are provided in Table 1. Phenolic compounds were chosen based on their common occurrence in waste streams, varying hydrophobicity and acidity depending on substituents, and ability to be oxidized by both DET and OH• oxidation pathways. Aliphatic acids were chosen because of their hydrophilic properties and they are common oxidation products of both AOPs and EAOPs due to low reactivity with OH•.

PFCs were chosen because they are hydrophobic compounds that are recalcitrant to biological and chemical degradation, nonreactive with OH^\bullet , and EAOPs are one of only few technologies that can destroy these compounds via DET reactions.

The conclusions of the various studies focused on organic compound oxidation at EAOP electrodes differ and interpreting the data is complicated by the fact that many studies did not eliminate mass transfer effects and likely were working at current densities near or exceeding the limiting current density, which is defined as a current density greater than that corresponding to a reaction/current controlled process. Therefore conclusions made from the studies are based on a combination of kinetic and mass transfer effects, as well as competition from intermediates formed during the reaction. Therefore, the discussion that follows reflects the pathways of electrochemical oxidation as in pertains to "real" treatment systems, which are often operated in the mass-transport or mixed control regime.

Table 1. List of various organic compounds and their key chemical properties.

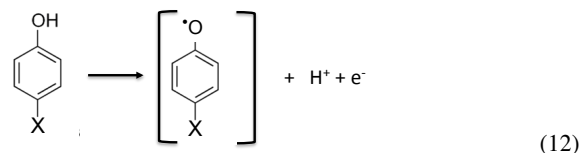
Chemical Class	pKa	Log K_{ow}	Hydroxyl Radical Rate Constant ($\text{L mol}^{-1} \text{s}^{-1}$)
Phenolic Compounds			
Phenol	10	1.44	6.6×10^9
2-chlorophenol	8.56	2.19	1.2×10^{10}
3-chlorophenol	9.12	2.48	7.2×10^9
4-chlorophenol	9.41	2.42	7.6×10^9
p-nitrophenol	7.15	1.91	3.8×10^9
p-methoxyphenol	10.2	1.34	2.6×10^{10}
1,4-benzoquinone	--	0.2	1.2×10^9
p-methylphenol	10.19	1.93	1.2×10^{10}
p-hydroxybenzaldehyde	7.72	1.11	1.0×10^{10}
Resorcinol	9.32, 11.1	0.8	1.2×10^{10}
Aliphatic Acids			
Formic	3.75	-0.54	1.3×10^8
Acetic	4.75	-0.25	1.6×10^7
Glyoxilic acid	3.18	-1.4	3.6×10^8
Glycolic acid	3.83	-1.07	6.0×10^8
Oxalic	1.25, 3.81	-0.81	1.4×10^6
Maleic	1.92, 6.23	0.46	6.0×10^9
Succinic	4.21, 5.64	-0.59	3.1×10^8
Malic	3.4, 5.11	-1.26	7.3×10^8
Malonic acid	2.85, 5.70	-0.81	2.0×10^7
Fumaric	3.02, 4.38	-0.48	6.0×10^9
Perfluorinated Organics			
Perfluorooctanoic Acid (PFOA)	3.8	a	NR
Perfluorooctanesulfonic Acid (PFOS)	-3.3	a	NR
Perfluorobutanesulfonic Acid (PFBS)	-4.99	a	NR

a = Log K_{ow} is not measurable by standard methods.
NR = no reaction

B.1. Phenols. Phenols are organic pollutants found in the effluents of oil refineries, production of pesticides and herbicides, dyes and textiles, pharmaceuticals, pulp and paper, plastics, and detergents. Conventional biological treatment is not suitable for the

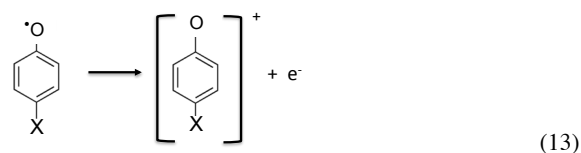
removal of these toxic and bio-refractory compounds. Therefore, a number of studies have investigated reaction mechanisms of various phenolic compounds on EAOP electrodes. Studies have focused on the electrochemical oxidation of various substituted phenols, including chlorinated phenols,^{7,8,15,30,34,138,204-211} p-substituted phenols (p-X, where X = H, OCH_3 , NO_2 , CH_3 , CHO),^{20,24,26,32,212} and multi-substituted phenols.^{15,213}

From the various studies reviewed it was found that three prevailing reaction pathways are thought to be prevalent for the oxidation of phenolic compounds on EAOP electrodes. These reaction pathways will be discussed using p-substituted phenols as model substrates and are summarized in Scheme 1. The first pathway is the formation of polymers, which is initiated by a DET reaction (Scheme 1, Pathway 1). This pathway is dominant at potentials less than that needed for significant OH^\bullet formation, which is in the electrode potential region of water stability (i.e., potential where anodic current does not flow in the background electrolyte). The DET mechanism has been inferred by CV experiments that show anodic current peaks associated with the addition of phenolic compounds to solution. The general reaction for a one-electron transfer step is shown in equation (12).

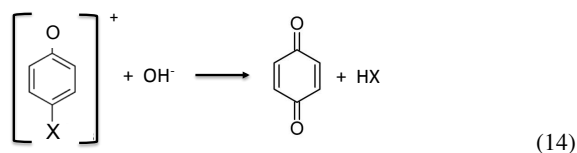


where X represents a constituent, shown in the para position. The phenoxyl radicals produced in reaction (12) can undergo polymerization reactions that form passivating films on the anode surface. Phenoxyl radicals form at anodic potentials $\sim > 0.5 \text{ V/SHE}$.²¹⁴ Studies suggest that polymer films are formed readily through C-C coupling or ether linkages between the radicals formed.^{215,216} Work has shown that polymer formation is also a function of the substituent type and number,^{15,215,216} which is likely due to electronic and steric effects. The electrochemical polymerization and subsequent adsorption of phenols from solution has also been utilized as a treatment strategy.^{20,217,218}

The second prevailing mechanism is characterized by the formation of p-BQ (Scheme 1, pathway 2). This mechanism is initiated by a second DET reaction involving the phenoxyl radical formed in equation (12).



Due to either competition from water oxidation at high potentials or thermodynamic limitations (i.e., high activation energies) the second DET reaction (equation (13)) is not significant for specific compounds, and this scenario has limited the use of active electrodes for the treatment of phenolic compounds, as OH^\bullet are needed to avoid electrode passivation through continual oxidation of the surface polymeric film.^{12,14,20,219,220} The phenoxonium ion formed in equation (13) is rapidly converted to p-benzoquinone (p-BQ) via nucleophilic attack by water, and subsequent release of the substituent, as shown in equation (14).



Various studies have shown near quantitative conversion of p-substituted phenols to p-BQ at potentials less than that needed for sufficient OH^\bullet production.^{3,9,221} The reason for this selective conversion is that p-BQ does not undergo DET reactions at the anode surface,¹⁹ and only degrades via OH^\bullet oxidation ($k_{\text{OH}^\bullet, \text{p-BQ}} = 1.2 \times 10 \text{ M s}^{-1}$).¹ Therefore, EAOP electrodes are often needed for the complete mineralization of phenolic compounds when significant concentrations of p-BQ are formed.¹²

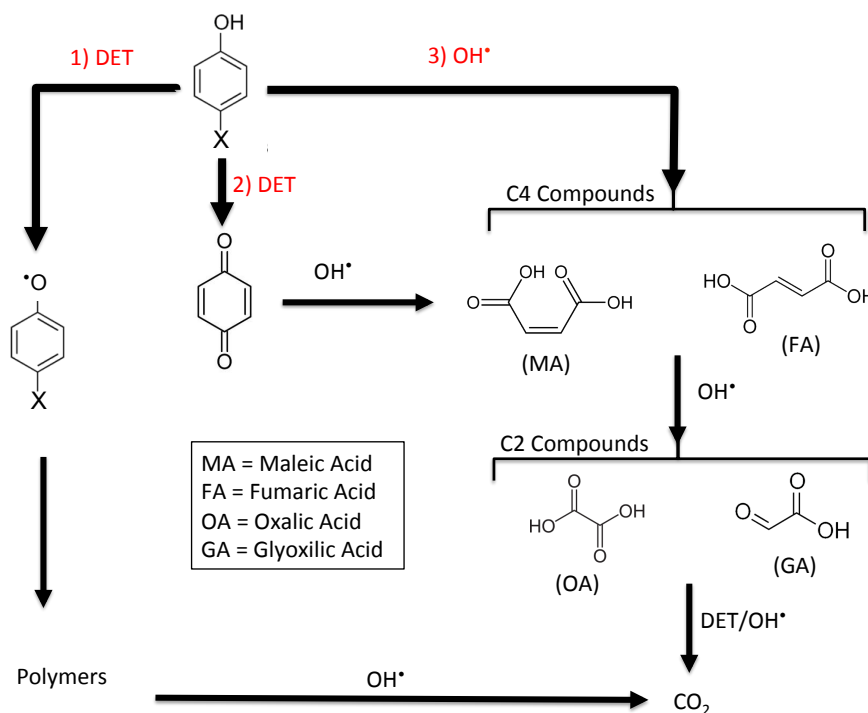
The third prevailing pathway for phenolic compound oxidation on EAOP electrodes is via reaction with OH^\bullet either adsorbed on the electrode surface or in the anode diffuse layer (Scheme 1, pathway 3). It is well documented that OH^\bullet react at near diffusion-limited rates with a wide range of phenolic compounds, as shown in Table 1. This mechanism is dominant in the potential range of water decomposition, where significant quantities of OH^\bullet are formed. The exact location of OH^\bullet attack on phenolic compounds varies dependent on substituent type, location, and quantity, as well as electrode type.^{4,10,222} Most studies have tried to elucidate the location of OH^\bullet attack via intermediate concentration profiles, but this is difficult due to the fact that intermediates are oxidized at different rates, so the most abundantly detected intermediate may not be the dominant one, but instead the intermediate with the slowest oxidation kinetics. Nevertheless, this information coupled to theoretical calculations have suggested that the charge of the C atom is an important determinant as to the location of OH^\bullet attack.²²² The primary intermediates observed in solution include C4 compounds (e.g., maleic, fumaric, and succinic acids) and C2 compounds (e.g.,

oxalic and glyoxylic acids).^{14,208,223,224} The C2 compounds are eventually mineralized to CO_2 through a combination of DET and OH^\bullet reactions.^{125,225,226}

Although phenolic compounds are well studied, discrepancies exist on the prevailing oxidation mechanism on different EAOP electrodes. Several studies have observed that Hammett constants are an indication of p-substituted phenolic compound reactivity.^{24,32,227} It was reported that the Hammett constant of p-substituted phenols correlated with measured rate constants on BDD electrodes, with more electron withdrawing groups correlated with higher rates of OH^\bullet reaction.^{24,32} Studies on various other doped- SnO_2 electrodes reported that the measured rate constants for the oxidation of p-substituted phenols correlated with a combination of the Hammett constant, initial surface concentration, and various other molecular descriptors.^{24,227} A closer look at these various correlations indicates that linearity was highly correlated to the reported rate constant for p- NO_2 ,²⁴ which was always much higher than for the other p-substituted phenols.^{24,32,227} These studies were conducted at high applied current densities (i.e., 20–100 mA cm^{-2}), which suggests mass-transport limitations, and in undivided cells where compound reduction was possible.^{24,32,227} Studies have shown that p- NO_2 is easily reduced to p- NH_2 by cathodic reactions,^{212,228} which may have contributed to the faster reaction rates of p- NO_2 and obscured the intrinsic reaction rate trends that were desired in these studies.^{24,32,227}

By contrast when the anode and cathode were divided by a Nafion® membrane and reaction rates were kinetically limited, p-NP oxidation was slightly lower than p-MP on BDD electrodes,²⁷ as would be predicted by reaction rate constants with OH^\bullet (Table 1). A similar result was observed during the oxidation of p-NP and p-MP on Sb-doped SnO_2 anodes in a divided cell reactor.³³ Mathematical kinetic models based on Langmuir-Hinshelwood kinetics determined that the zero-order apparent reaction rate constant was higher for p-

Scheme 1. Proposed pathways for the electrochemical oxidation of p-substituted phenols.



MP ($1.84 \times 10^{-3} \text{ mol L}^{-1} \text{ s}^{-1}$) compared to p-NP ($2.35 \times 10^{-4} \text{ mol L}^{-1} \text{ s}^{-1}$) on a Bi-doped PbO_2 electrode.²²⁹

Mass transport may also have a substantial affect on the prevailing reaction mechanism. In the absence of mass transport control, substrates accumulate on the electrode surface and thus allow both DET and OH^\bullet oxidation to occur simultaneously (Scheme 1, Pathways 1-3). Under mass transport control and for fast reacting substrates, the substrate is degraded in the diffuse zone and is completely depleted before it reaches the anode surface, and thus the DET reaction cannot occur.²⁷ For this situation only Pathway 3 in Scheme 1 would be relevant. Many of the discrepancies related to phenolic compound oxidation in various studies may be related to differences in mass transport rates. Unfortunately, most studies do not report mass transfer rate constants, so it is difficult to make a conclusion on this topic. Based on the discussion above, it is suggested that future electrochemical research be mindful to eliminate diffusion limitations and conduct reactions in divided cells when mechanistic or intrinsic kinetic data is desired on a single electrode. However, many electrochemical processes utilize undivided cells, and kinetic studies of these systems are also important to further process optimization.

B.2. Aliphatic Acids. As shown in Scheme 1 EAOPs result in the production of various aliphatic acids (e.g., maleic, fumaric, oxalic, and glyoxilic acids). These compounds tend to accumulate in solution because they have $k_{\text{OH}^\bullet, \text{R}}$ values 1 to 3 orders of magnitude lower than phenolic and aromatic compounds (Table 1). Various studies have been conducted that studied the electrochemical oxidation of aliphatic acids at EAOP electrodes.^{20,109,125,179,226,230-244} While the complete mineralization of aliphatic acids is possible at EAOP electrodes, it requires high electrical charges and reaction times, and thus increases the cost of electrochemical treatment. EAOP electrodes have been shown to be more reactive to aliphatic compounds compared to other AOPs due to the DET pathway,²⁴⁵ which is initiated by the formation of a RCOO^\bullet intermediate that decarboxylates via the Kolbe electrolysis mechanism.

The aliphatic acids of most interest to researchers are oxalic and acetic acid, as these compounds are representative of assimilated organic carbon that is produced during oxidative processes,^{246,247} which can cause biological growth during water reuse.²⁴⁸ The accumulation of these compounds during traditional AOPs is due to their low $k_{\text{OH}^\bullet, \text{R}}$ values (Table 1). These compounds are more reactive using EAOPs, due to the DET pathway, but are still observed to accumulate in solution during the oxidation of organic wastes.^{14,208,223,224} The persistence of acetic acid as an intermediate of organic compound oxidation is attributed to its lack of significant electrochemical activity via DET reactions,²⁴⁹ its inhibitory effect on OH^\bullet production,²⁵⁰ and its relatively low reaction rate constant with OH^\bullet ($k = 1.6 \times 10^7 \text{ M}^{-1} \text{ s}^{-1}$).¹ The electrochemical oxidation of acetic acid on BDD electrodes was studied and it was observed that acetic acid adsorbs to the BDD surface, likely via a DET reaction.²⁵⁰ Evidence suggests that the adsorbed acetic acid is not active for further DET reactions and its slow oxidation is attributed primarily to reaction with OH^\bullet .²⁴⁹ However, the adsorption of acetic acid at the electrode surface causes an autoinhibition of its oxidation through a displacement of H_2O at the anode surface and thus a decrease in OH^\bullet production.²⁵⁰ Acetic acid has also been shown to inhibit the oxidation of other compounds that undergo DET reactions.²⁵⁰ In light of the slow oxidation of acetic acid on EAOP electrodes, complete mineralization of complex waste streams is obtained, due to alternative pathways that do not produce acetic acid as an intermediate (e.g., see Scheme 1).

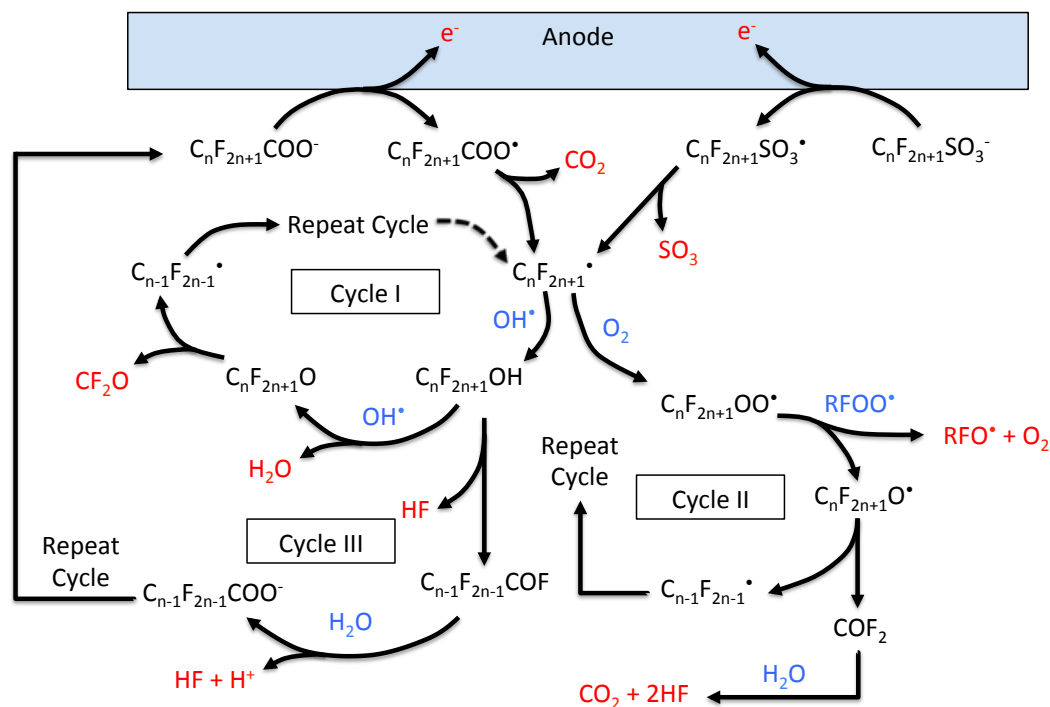
Oxalic acid has a very low rate constant with OH^\bullet ($k_{\text{OH}^\bullet, \text{R}} = 1.4 \times 10^6$),¹ which results in its accumulation and low removal rates during EAOPs. Studies have shown that oxalic acid is removed by a DET mechanism at BDD, doped- SnO_2 , PbO_2 , and Ti_4O_7 electrodes.^{20,125,226,241} The oxidation of oxalic acid occurred at lower overpotentials at doped- SnO_2 electrodes compared to BDD and Ti_4O_7 electrodes,^{20,125} which may suggest surface promoting effects at doped- SnO_2 electrodes. Oxalic acid oxidation is highly sensitive to the surface functional groups present at the BDD surface.¹⁷⁹ It was shown that a hydrogen-terminated surface results in the oxidation of oxalic acid at lower overpotentials relative to an oxygen-terminated surface,¹⁷⁹ providing further evidence that oxalic acid oxidation is surface sensitive.

B.3. Perfluorinated Organic Compounds. Perfluorinated organic compounds (PFCs) have been used extensively in metal plating, semiconductor manufacturing, and a variety of household goods.²⁵¹ Due to high stability of the carbon-fluorine bonds,²⁵² PFCs are recalcitrant to chemical and biological reactions. As a result, PFCs have accumulated in the environment and the human body.²⁵³⁻²⁶⁴ While PFCs are resistant to traditional AOPs,^{265,266} various studies have shown that they are effectively degraded by EAOPs.^{5,16,39,40,42,267,268}

The reaction mechanism of PFC oxidation on EAOP electrodes was first investigated by Carter and Farrell,¹⁶ who studied the oxidation of perfluorooctane sulfonate (PFOS) at BDD electrodes. A combination of experimental and DFT modeling studies was used to determine the rate-limiting mechanism for PFOS oxidation. It was concluded that the oxidation of PFOS was initiated by a direct electron transfer at the anode surface that became activationless at potentials $\geq 2.7 \text{ V/SHE}$.¹⁶ In a similar study, it was concluded through DFT simulations that perfluorobutane sulfonate (PFBS) underwent a direct electron transfer at the anode surface that became activationless at potentials $\geq 3.0 \text{ V/SHE}$.³⁹ Experimental results from other studies showed that PFOA oxidation only occurred at anodic potentials $\geq 3.37 \text{ V/SHE}$ at SnO_2 -Sb-Bi/Ti anodes⁵ and $\geq 3.0 \text{ V/SHE}$ at BDD anodes.²⁶⁷ These potentials agree well with those determined by DFT simulations,^{16,39} thus supporting the validity of the modeling results. The slightly lower anodic potential necessary for oxidation at BDD anodes relative to SnO_2 -Sb-Bi/Ti anodes may be related to the greater hydrophobicity of BDD relative to SnO_2 -Sb-Bi/Ti anodes, but more data is necessary to make a conclusive statement.

Experimental results showed an empirical trend during the oxidation of perfluoro-acids and perfluoro-sulfonates, where the observed reaction rate constants increased with increasing C atoms.⁴⁰ These results suggest that the number of carbons in the PFC may affect the anodic potential needed to extract an electron. As the C:F ratio in the PFC increases (i.e., longer chain length), the electron density of the functional group (e.g., $-\text{SO}_3$) should increase, and thus lower the energy needed for direct electron transfer to the anode. DFT modeling supports this hypothesis, as the oxidation of PFOS and PFBS were calculated to be activationless at potentials ≥ 2.7 and $\geq 3.0 \text{ V/SHE}$, respectively.^{16,39} As a result, shorter chained PFC intermediates have been observed to accumulate at mg L^{-1} levels during anodic oxidation.^{5,16,39,40,267}

A detailed mechanism regarding PFOA oxidation was proposed based on results from PFOA oxidation in $\text{H}_2(^{18}\text{O})$, and the authors proposed two routes for PFOA oxidation, both of which are initiated by a DET reaction.⁵ Recent DFT modeling suggested slight modifications to the reaction mechanism proposed by Zhuo et al.,⁵ based on activation energy calculations.⁴² The proposed mechanism

Scheme 2. Proposed pathways for the electrochemical oxidation of PFCs.

for PFC oxidation is illustrated in Scheme 2. Experimental work suggests that perfluoro-sulfonates release their functional group at the same rate as parent compound degradation and are rapidly converted to perfluoro radicals,^{39,267} thus the pathway shown in Scheme 2 incorporates both perfluoro-acids and perfluoro-sulfonates. After the DET step, the PFC radical releases its functional group to form a perfluoro radical ($C_nF_{2n+1}\cdot$). Cycle I in Scheme 2 shows the most energetically favorable reaction pathway, as determined by DFT model simulations (all activation energies $< 35 \text{ kJ mol}^{-1}$).⁴² In Cycle I the $C_nF_{2n+1}\cdot$ compound reacts with $OH\cdot$ formed on the anode and subsequently releases H_2O to form $C_nF_{2n+1}O$, which then releases CF_2O to form a perfluoro radical with one C atom removed ($C_{n-1}F_{2n-1}\cdot$). The cycle continues, yielding progressively shorter chained perfluorinated compounds, until complete mineralization occurs. This pathway is consistent with experimental studies that detected small quantities of intermediates during the electrochemical oxidation of PFCs.^{16,39,42}

Various studies have detected low levels of shorter chained perfluoro acid intermediates during the electrochemical oxidation of PFCs,^{5,16,39,40,42,267,268} indicating other oxidation mechanisms must be present. Cycle II in Scheme 2 shows a different pathway, where the $C_{n-1}F_{2n-1}COF$ compound releases HF to form $C_{n-1}F_{2n-1}COF$, which then undergoes hydrolysis to form a perfluoro acid with one C atom removed ($C_{n-1}F_{2n-1}COO\cdot$). The cycle continues, yielding progressively shorter-chained perfluoro acids. Theoretical DFT calculations indicate that the initial step of HF release is associated with a high activation barrier (i.e., 223 kJ mol^{-1}).⁴² The fact that shorter chained perfluoro acid intermediates have been detected experimentally suggests that catalytic effects at the electrode surface may be involved, or the existence of other unidentified pathways for their formation.

PFOA oxidation in $H_2(^{18}O)$ has also provided evidence for a third mechanism for PFC oxidation,⁵ which is illustrated in Cycle III

of Scheme 2. Once $C_nF_{2n+1}\cdot$ is formed it may react with dissolved O_2 to form a peroxy radical species. This radical can react with other peroxy radicals to yield an intermediate alcohol radical $C_nF_{2n+1}O\cdot$ which decays to form an alkyl radical with one C atom removed ($C_{n-1}F_{2n-1}\cdot$). The $C_{n-1}F_{2n-1}\cdot$ molecule is then able to further react in Cycles I, II, and III. DFT studies have also suggested that perfluoro radicals can react with water via a H-atom abstraction mechanism.⁴² However, the calculated activation energy is high (55 kJ mol^{-1}) and experimental evidence does not exist supporting its occurrence. Therefore, it was not included in Scheme 2.

Studies have shown near complete TOC removal during anodic oxidation of PFCs, but F mass balances between only 75–92% have been reported,^{5,16,39,42} suggesting volatile losses of HF and trifluoroacetic acid may be occurring.^{5,16,39} The mechanisms outlined in Scheme 2 do not account for trifluoroacetic acid (TFA) oxidation. The mechanism for the electrochemical removal of TFA has not been investigated, but likely involves a combination of volatilization, DET reactions, and reaction with $OH\cdot$. However, the reaction rate between TFA and $OH\cdot$ is low, as the measured rate constant is $1.0 \times 10^5 \text{ M}^{-1} \text{ s}^{-1}$.²⁶⁹

C. Rate Limitations in Applied Settings

Either chemical or mass transport processes limit contaminant oxidation rates. Chemical processes include adsorption, electron transfer, bond breaking/making, and structural reorganization. Mass transport processes include diffusion, migration, or advection to the electrode surface. Although the actual electron transfer step is extremely fast ($\sim 10^{-16} \text{ s}$), the reorganization of the structure of the reactants and products is slower ($10^{-11} - 10^{-14} \text{ s}$) and ultimately dictates measured rate constants. The largest measured surface area normalized rate constants (k_a) are in the range of 0.01 to 0.1 m s^{-1} .²⁷⁰ However, many reactions are more complicated and involve significant molecular rearrangement upon electron transfer, and thus much lower k_a values have been reported. For example, a k_a value of

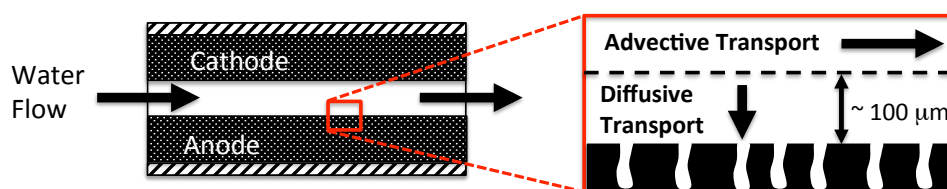
$2.36 \times 10^{-4} \text{ m s}^{-1}$ for the oxidation of the disinfection byproduct *N*-nitrosodimethylamine on BDD electrodes has been reported.²⁸ The reaction of substrates with OH^\bullet are often in the diffusion limited range with second order rate constants commonly ranging from 10^9 to $10^{10} \text{ M}^{-1} \text{ s}^{-1}$.¹ Experimental and modeling studies have also shown that due to the high reactivity of OH^\bullet , they exist in only a narrow zone adjacent to the electrode surface ($< 1.0 \mu\text{m}$).^{25,27,271} As a result of these very fast kinetic processes and small reaction zone volumes the operation of EAOP technologies become mass transport limited at relatively low applied current densities (e.g., $< 5 \text{ mA cm}^{-2}$).^{27,272} Most studies are therefore operated under mass transport limited conditions, where reaction rates are governed by the diffusion of contaminants to the electrode surface. Therefore, current research is focused on the development of high active surface area electrodes that utilize strategies to maximize mass transport rates.

Traditional reactors for EAOP technologies utilize parallel plate

operated in parallel plate flow by-mode, as features of electrode roughness that are smaller than the diffusion length become averaged into the diffusion field.²⁷⁰

In order to overcome diffusional limitations in electrode systems, research has focused on the use of porous flow-through electrodes, as shown in Figure 2b. This reactor type utilizes a porous electrode in the form of a filter or membrane, and water is advected through pores that are on the order of $0.1\text{--}1.0 \mu\text{m}$ wide.^{20,273,274} The advantage of this technique is that a high specific surface area of electrode is active for electrochemical reactions,²⁰ and the very small pore diameters prevent radial diffusion limitations.^{20,274} As a result of flow-through operation, electrochemical carbon nanotube flow-through reactors showed a 2- to 6-fold increase in k_m values relative to their batch systems,^{273,274} and values for k_m as high as $1.7 \times 10^{-5} \text{ m s}^{-1}$ were reported.²⁷³ However, carbon nanotubes are not active for OH^\bullet production and therefore recent work has deposited doped-

a) Flow-by Electrode Operation



b) Flow-through Electrode Operation

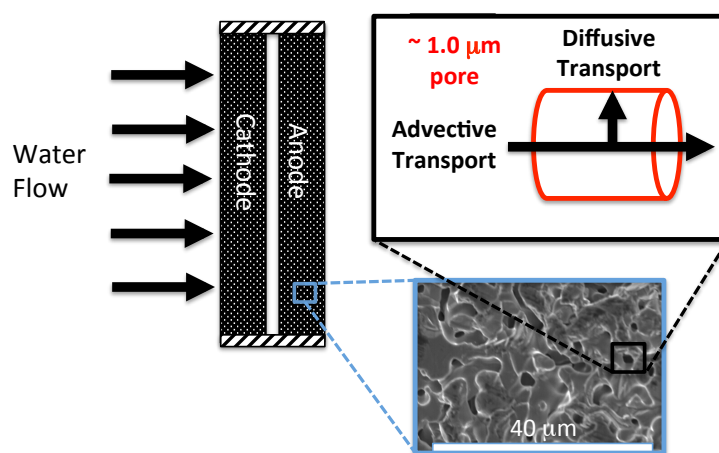


Figure 2. Schematics showing: a) Flow-by electrode operation, where contaminants most diffuse through a $\sim 100 \mu\text{m}$ thick diffusion zone to reach the anode surface. Inset shows a schematic of the diffuse zone adjacent to the electrode surface. b) Flow-through operation, where water is advected through a $\sim 1.0 \mu\text{m}$ pore and thus most only diffuse radially to the pore wall to react. Insets show an SEM image of a porous Ti_4O_7 electrode and a schematic of a single pore.

reactors operated in flow-by mode, as shown in Figure 2. These reactors contain anodes and cathodes that are separated by narrow flow channels (in the mm to cm range), and waste solution is pumped through these channels in either one-pass or recirculation mode. Reaction rates are governed by the diffusion of substrates through a thin stagnant boundary layer ($\sim 100 \mu\text{m}$) that develops at the electrode surface (diffusion layer), as shown in Figure 2a. This boundary layer is a function of the cross-flow velocity and the turbulence of the flow. With the use of parallel plate electrodes, surface area normalized mass transfer rate constants (k_m) on the order of $10^{-6}\text{--}10^{-5} \text{ m s}^{-1}$ are attainable.²⁷² High surface area electrodes only result in modest increases in oxidation rates when

SnO_2 catalysts on carbon nanotubes in order for them to function as an EAOP electrode.¹⁰⁹ Recent work with a Ti_4O_7 electrode showed that advection-enhanced mass transport resulted in a 10-fold increase in mass transport rate constants using flow-through compared to flow-by operation, with a k_m value of $2.6 \times 10^{-5} \text{ m s}^{-1}$ reported.²⁰ It has also been shown that operation in a flow-through mode results in advection-limited mass transport.²⁰ Therefore, very high reaction rates are conceivable in these systems if high porosity flow-through electrodes are developed that allow minimal back-pressure during flow-through operation. Flow-through electrode development is an expanding area of research,^{20,109,275} which has the possibility of significantly contributing to advances in water treatment.

D. Long-term Sustainability

Before EAOPs can be considered a viable water treatment technology, their long-term sustainability must be assessed. Important to this assessment is quantifying the performance of EAOPs in applied treatment settings and the negative environment impacts that may arise from their use. To that end, an assessment of EAOPs to matrix effects, byproduct formation, and a comparison to traditional AOPs using performance and environmental measures is provided.

D.1. Matrix Effects. Similar to traditional AOPs, substrate degradation rates during EAOPs are affected by solution conditions. Since OH^\bullet are nonselective reactants, the presence of natural organic matter (NOM) and other inorganic ions can result in reduced reaction rates of the target substrate. In general, the effect of non-target water constituents on target compound oxidation can be estimated by the following expression:

$$R_R = \frac{k_{R,\text{OH}^\bullet} C_R}{k_{R,\text{OH}^\bullet} C_R + \sum k_{i,\text{OH}^\bullet} C_i} \quad (15)$$

where R_R is the relative reaction rate with the target compound, k_{R,OH^\bullet} is the second-order reaction rate constant of R with OH^\bullet , k_{i,OH^\bullet} is the second-order reaction rate constant of the i^{th} compound with OH^\bullet , and C_R and C_i are aqueous concentrations. A list of common OH^\bullet scavengers and their reported k_{i,OH^\bullet} values are provided in Table 2. Since the structure of NOM is undefined and can vary between water sources, a range of $k_{\text{NOM},\text{OH}^\bullet}$ values are reported.²⁷⁶ When treating natural waters, carbonate species, chloride, and NOM can have the biggest influence on target compound oxidation, as they are often present at higher concentrations than the target compound.

Table 2. Common hydroxyl radical scavengers and their respective reaction rate constants.

Compound	Hydroxyl Radical Rate Constant (L mol ⁻¹ s ⁻¹)
H ₂ CO ₃	< 1.0 × 10 ⁶
HCO ₃ ⁻	8.5 × 10 ⁶
CO ₃ ²⁻	3.9 × 10 ⁸
Cl ⁻	4.3 × 10 ⁹
Fe(II)	3.3 × 10 ⁸
NOM	1.4-4.5 × 10 ⁸

The primary difference between EAOPs and traditional AOPs with regard to scavenging by non-target water constituents is related to the acidic diffusion boundary layer that is generated on the anode surface due to water oxidation (equation 1). Coupling the Faraday's law of electrolysis equation with Fick's first law of diffusion provides an equation to predict the surface concentration (C_s) of H^+ at the anode surface.

$$C_s = C_B + \frac{\alpha j}{n F k_m} \quad (16)$$

where C_B is the bulk concentration, j is the applied current density, n is the number of electrons transferred (in this case $n = 1$), F is the Faraday constant, k_m is the mass transport coefficient, and α is the fraction of current going towards the reaction of interest. Assuming that all current is directed towards water oxidation (i.e., $\alpha = 1$), the

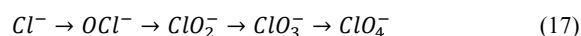
bulk $\text{pH} = 7.0$, $k_m = 10^{-6} \text{ m s}^{-1}$, and $j = 10 \text{ A m}^{-2}$; the pH at the electrode surface in an unbuffered electrolyte is estimated at < 1.0 .

This acidic diffuse zone has been shown to limit OH^\bullet scavenging by HCO_3^- , due to the rapid protonation of HCO_3^- and conversion to H_2CO_3 ($k = 1 \times 10^{10} \text{ M}^{-1} \text{ s}^{-1}$)²⁷⁷ relative to the reaction between OH^\bullet and HCO_3^- ($k = 8.5 \times 10^6 \text{ M}^{-1} \text{ s}^{-1}$).²⁹ Since H_2CO_3 is effectively nonreactive with OH^\bullet (Table 2), it was shown that reaction rates of NDMA were not affected by the presence of a 5 mM HCO_3^- concentration.²⁹ Studies using the $\text{O}_3/\text{H}_2\text{O}_2$ AOP, showed that NDMA oxidation rates declined significantly in the presence of HCO_3^- at concentrations $> 1 \text{ mM}$.²⁷⁸ Results from studies using the UV/TiO₂ photocatalyst to degrade organics in reverse osmosis concentrates indicated that the water had to be acidified to $\text{pH} = 5$ in order to obtain oxidation of the organic compounds, due to OH^\bullet scavenging by HCO_3^- present at neutral pH . These results indicate that the acidic diffuse zone that develops on the anode surface provides a key advantage towards compound oxidation compared to other AOPs, which allows EAOP technologies to effectively treat organics present in carbonate-containing waters. Since all natural waters contain carbonate species, this advantage is a significant improvement over traditional AOPs.

D.2. Byproduct Formation. Until recently toxic byproduct formation has not been addressed during the operation of EAOPs. However, the formation of ClO_4^- during the electrochemical oxidation of chloride-containing water is not surprising, as industrial synthesis of ClO_4^- is accomplished by the oxidation of ClO_3^- solutions with PbO_2 and Pt anodes.²⁷⁹⁻²⁸³ Recent work has shown that the oxidation of chloride on BDD electrodes can form ClO_4^- ²⁸⁴⁻²⁸⁸ and chlorinated-organic compounds.^{45,46,51,289-291}

D.2.1 Perchlorate formation. The formation of ClO_4^- is especially problematic because it is a terminal oxidation product and its consumption has been linked to health risks.^{292,293} As a result of these health risks, the EPA has issued a health advisory level of $15 \mu\text{g L}^{-1}$ for drinking water sources,²⁹⁴ and Massachusetts and California have set drinking water standards of 2 and $6 \mu\text{g L}^{-1}$, respectively.^{295,296}

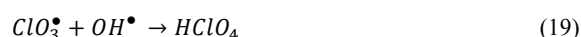
Previous research has shown that ClO_4^- forms via a multistep oxidation pathway starting from chloride, as shown in equation (17):



where the rate-determining step is the oxidation of ClO_3^- to ClO_4^- .^{284,297} Experimental and DFT modeling studies have shown that the conversion of ClO_3^- to ClO_4^- on BDD anodes is a two-step process.²⁰⁰ The first step associated with ClO_4^- formation is a DET reaction between ClO_3^- and the electrode surface (equation (18)).²⁰⁰



The second step involves a homogeneous reaction between ClO_3^\bullet and OH^\bullet to form HClO_4 (equation (19)).²⁰⁰

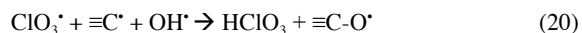


Work by Azizi et al.²⁰⁰ was conducted under kinetic-control and in the absence of other competing species (e.g., OH^\bullet scavengers); under these conditions it was found that equation (18) was the rate-determining step for ClO_4^- formation.

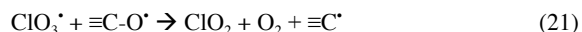
Studies focused on the formation of ClO_4^- on other EAOP electrodes under relevant water treatment conditions could not be found. However, work by Bergmann et al.²⁸⁵ showed that ClO_4^-

formation on BDD electrodes is approximately 50 to 100 times higher than on Pt and mixed-metal oxide electrodes. These results are consistent with the fact that OH^\bullet are not formed at high quantities on active electrode materials. However, recent work has suggested that the various functional groups present on the BDD surface may also contribute to ClO_4^- formation.^{200,298} As shown in Figure 1 and discussed previously, freshly synthesized BDD electrodes are hydrogen terminated ($\equiv\text{C-H}$ and $\equiv\text{CH}_2$), but once subjected to anodic polarization various oxygenated and oxygenated radical groups can form. Under anodic conditions the removal of an electron from these functional groups can form surface radical sites. DFT modeling studies have determined that the surface radical sites can act as adsorption sites for ClO_x^\bullet radicals.^{200,298} Adsorption can stabilize the ClO_x^\bullet radicals and increase their life times, so as to increase their reaction rates with OH^\bullet .²⁹⁸ DFT modeling simulations indicate that the adsorption of ClO_x^\bullet species at BDD sites and their subsequent reaction with OH^\bullet occur with activation barriers $< 10 \text{ kJ mol}^{-1}$, indicating that they are significant reactions at room temperature.²⁹⁸

Interestingly, results from DFT modeling indicate that the reaction of ClO_3^\bullet at BDD surface sites may act to slow ClO_4^- formation.²⁰⁰ For example, the adsorption of ClO_3^\bullet at $\equiv\text{C}^\bullet$ sites and subsequent reaction with OH^\bullet produces ClO_3^- and an oxidized surface site, as shown in equation (20).



The reaction of ClO_3^\bullet at $\equiv\text{C-O}^\bullet$ sites produces ClO_2 , O_2 , and a carbon radical surface site, as shown in equation (21).



These reactions occur with low activation barriers ($< 28 \text{ kJ mol}^{-1}$), indicating that they are significant reactions at room temperature.²⁰⁰ The slower observed formation of ClO_4^- relative to other oxychlorine anions (e.g., ClO_2^- and ClO_3^-)²⁹⁹ may be related to these surface site effects.

It has been shown that the formation of ClO_4^- from ClO_3^- occurs significantly slower than the mass transfer rate, and therefore ClO_3^- accumulates at the electrode surface.²⁷ Therefore in the presence of OH^\bullet scavenging compounds, mass transport of these OH^\bullet scavengers has a substantial effect on ClO_4^- formation. Results from reactive-transport modeling of the diffuse layer adjacent to the anode surface indicate that ClO_4^- formation is controlled by the competition between organic compounds and ClO_3^\bullet for OH^\bullet within a reaction zone (0.02–0.96 μm) adjacent to the anode surface.²⁷ Therefore, mass transport of organic compounds to the electrode surface has a profound effect on ClO_4^- formation. Under kinetic-limited conditions, organics reach the anode surface and substrates with higher OH^\bullet reaction rates show greater inhibition of ClO_4^- formation. When organic compound oxidation becomes mass transfer-limited, they are degraded a small distance from the anode surface. Therefore, OH^\bullet scavenging does not occur at the anode surface and inhibition of ClO_4^- formation is minimal. These results show that controlling reactor conditions could potentially limit ClO_4^- production during EAOP treatment of organic compounds.

D.2.2 Halogenated Organic Compound Formation. Recently, the formation of halogenated-organic compounds (HOCs) have been detected during EAOPs.^{45,46,51,289-291} HOCs have been detected during the oxidation of organics in landfill leachate,⁵¹ reverse osmosis concentrates,^{45,46} and model aqueous systems.^{289-291,300} HOC formation is attributed to addition and substitution reactions between organic compounds and *in situ* formed active chlorine species (e.g.,

Cl_2 , OCl^\bullet , HOCl) and chlorine radicals (Cl^\bullet , Cl_2^\bullet).⁷⁶ General conclusions that can be made from these studies are that 1) HOCs are continuously formed during electrolysis while halogens and organics are both present, 2) HOCs can be completely oxidized to inorganic end products (i.e., CO_2 , ClO_3^- , ClO_4^- , BrO_3^-) after elimination of halogen ions or halogenated oxidants, and 3) the incorporation of halogens into organics increases in the following order $\text{Cl} < \text{I} < \text{Br}$.

The potential formation of individual HOCs is rather diverse and very few studies have investigated the topic in detail. Anglada et al.⁵¹ performed a detailed analysis of the HOCs formed during the treatment of landfill leachate with an EAOP using a BDD electrode flow-cell operated under mass transfer limitation and in differential batch mode. The landfill leachate had a COD concentration of 3385 mg L^{-1} and Cl^- and Br^- concentrations of 2587 and 9 mg L^{-1} , respectively. The formation of various HOCs was detected, including trihalomethanes (THMs), haloacetonitriles (HANs), haloacetones (HKs), and 1,2-dichloroethane (DCA). Chloroform was the primary HOC formed, and represented on average 55% of the total HOC concentration. HANs (primarily dichloroacetonitrile and bromochloroacetonitrile) comprised 19–25% of total HOCs. Some trends were observed for the formation of specific classes of HOCs. It was observed that the formation of HANs and HKs was enhanced at low pH. The formation of DCA increased with increasing pH, applied current densities, and chloride concentrations. The formation of THMs was relatively insensitive to changes in operational parameters. With the exception of DCA, HOCs increased in concentration with electrolysis time, and maximum concentrations of 1.9 mg L^{-1} , 753 $\mu\text{g L}^{-1}$, and 431 $\mu\text{g L}^{-1}$ were detected for THMs, HANs, and HKs, respectively, at an applied charge of 14.4 Ah L^{-1} . DCA was not detected at this applied charge, indicating it was oxidized to other products. Although high levels of HOCs formed after an applied charge of 14.4 Ah L^{-1} , their concentrations plateaued towards the end of the experiments, which corresponded to $\sim 50\%$ COD removal. Unfortunately, trends of chloride and its inorganic oxidation products (Cl_2 , OCl^\bullet , ClO_3^- , ClO_4^-) were not reported, which would allow an assessment of the relationship between these species and HOC formation. HOCs are expected to eventually be mineralized, as prior studies have shown halogenated-organics are efficiently oxidized on EAOP electrodes.^{43,241}

Studies have also detected HOC formation during EAOP treatment of reverse osmosis concentrates.^{45,46} Bagastyo et al.⁴⁵ investigated the formation of HOCs during the treatment of reverse osmosis concentrates using BDD anodes. Instead of characterization of a variety of individual HOCs, Bagastyo et al.⁴⁵ determined the formation of adsorbable organic chlorine (AOCl), adsorbable organic bromine (AOBr), and adsorbable organic iodine (AOI) compounds. Due to the relatively low concentration of Br^- (1.6 mg L^{-1}) and I^- (0.5 mg L^{-1}) in the RO concentrate, AOBr and AOI compounds formed but were degraded at higher applied charges. However, the very high chloride concentration (1386 mg L^{-1}) resulted in a continuous increase in AOCl concentration ($\sim 0.88 \text{ mM}$) until the end of the experiment (i.e. 10.9 Ah L^{-1}). In this same study, the formation of total trihalomethanes (tTHMs) and total haloacetic acids (tHAAs) was observed, both of which were degraded with an increase in applied charge, to final total concentrations between 1 and 4 μM (tTHMs), and 12 and 22 μM (tHAAs). The presence of HOCs during the entirety of these experiments was attributed to the presence of residual free available chlorine (FAC) (i.e. 25 and 270 mg L^{-1} at pH 1-2 and pH 6-7, respectively) and DOC ($\sim 15 \text{ mg C L}^{-1}$) at the end of these experiments. It appears that complete removal of FAC is necessary to completely eliminate chlorinated organic compound formation.

Bagastyo et al.⁴⁵ also found that Br⁻ and I⁻ were converted to halogenated products at much greater proportions (~100% and 50% molar concentrations, respectively) compared to Cl⁻ (~3%). This result is likely related to the higher reactivity of HOBr/OBr⁻ and HOI/OI⁻ species towards phenolic compounds,³⁰¹ and the possibility of stripping of chlorine into the gas phase, which is not as significant for the less volatile bromine and iodine species.

Further work by Bagastyo et al.⁴⁶ compared the relative formation of THMs and HAAs as a function of electrode type (Pt-IrO₂/Ti, SnO₂-Sb/Ti, BDD) and electrolyte composition (NaCl, NaNO₃, and Na₂SO₄). In these studies it was found that HAA and THM production was highest for the BDD electrode in the 0.05 M NaCl electrolyte, although Ti/Pt-IrO₂ was the most effective electrode for the production of free available chlorine.⁴⁶ These results may be attributed to the interaction of BDD surface sites with halogenated radical and organic species. The functional groups on the BDD surface may stabilize these radicals, which would promote their relative lifetimes and increase the probability for reaction. It was also found that the production of THMs and HAAs on BDD electrodes was an order of magnitude higher in the Na₂SO₄ electrolyte compared to the NaNO₃ electrolyte (Cl⁻ = 4 mM for both).⁴⁶ This result may be due to the production of S₂O₈²⁻ or SO₄^{•-} at the BDD electrode during anodic treatment.^{302,303} These *in situ* formed oxidants may enhance Cl⁻ oxidation and thus formation of HOCs. Interestingly, the BDD anode showed the lowest production of HAAs and THMs of the three electrodes in the NaNO₃ electrolyte.⁴⁶ The reason for this result is unclear, but may be related to increased adsorption of NO₃⁻ at the BDD anode surface relative to the other electrodes. This adsorption has the possibility of blocking reaction sites for DET reactions.

The oxidation of different organic compounds (0.5 mM) (resorcinol, dimethyl phthalate, diethyl phthalate, bisphenol-A) in the presence of 10 mM chloride was used to evaluate the formation of chloroform under constant current (20 mA cm⁻²) conditions.³⁰⁴ It was observed that chloroform formation was approximately an order of magnitude higher in the presence of resorcinol compared to other model organic compounds.³⁰⁴ The high production of HOCs during the electrolysis of resorcinol in the presence of chloride is related to the activity of the ortho-position carbon atom towards electrophilic addition of chlorine atoms.³⁰⁵ During chlorination of resorcinol containing water, large quantities of monochloro-resorcinol and dichloro-resorcinol were detected followed by hydrolysis to form chloroform.^{306,307} The relative formation of chloroform during electrolysis of resorcinol should be a good indicator of chlorinated byproduct formation potential during the electrolysis of natural waters containing chloride, as resorcinol is a good surrogate that represents the functional groups present in NOM.³⁰⁸

D.3. Performance Comparison and Life Cycle Analysis.

Little work has been dedicated to analyzing the cost and quantifying the environmental impacts of EAOPs. Recently, a cost and performance comparison between traditional oxidation processes and BDD electrodes for the treatment of a variety of water contaminants was performed.⁸⁵ In this study EAOP treatment with BDD electrodes, ozonation, and Fenton oxidation were compared. Several key findings from this study suggest that BDD electrodes can be competitive with traditional AOPs. It was found that EAOP was able to more completely mineralize various organic compounds as compared to ozonation and Fenton oxidation, without the accumulation of refractory compounds, and the efficiency of EAOP oxidation increased at higher contaminant concentrations, due to minimization of mass transport effects to the electrode surface. The cost of oxidant generation for BDD electrodes was less than

ozonation and comparable to Fenton oxidation. However, it was also observed that the individual organic compound had a large influence on operating costs. For all compounds oxidized, ozonation had the highest operating costs and overall the Fenton process had the lowest. However, EAOP could compete with the Fenton process during the treatment of acidic wastes and real wastewaters. This result is likely related to the presence of aliphatic acids that have low reaction rates with OH[•], and EAOP could more efficiently oxidize them due to the DET pathway. The initial capital investment required for BDD electrodes was less than ozonation but higher than Fenton oxidation due to the current cost of BDD electrodes. However, optimal Fenton operation has a tight pH regime and also produces high volumes of Fe sludge.⁸⁵

Only one study could be found that compared the environmental impacts of EAOPs and AOPs using a life cycle assessment (LCA) methodology.⁸⁰ In this study the environmental impacts of treating olive mill wastewater were assessed using electrochemical oxidation with BDD electrodes, wet air oxidation using a high-pressure reactor, and photocatalytic oxidation using a UV/TiO₂ reactor.⁸⁰ The main system inputs that were analyzed included energy inputs (electricity used), laboratory reactors, and additional materials and chemicals used for treatment. The impacts of the three processes were normalized by the removal of 1 g L⁻¹ chemical oxygen demand (COD) and 1 g L⁻¹ of total phenol. Due to the relatively long life spans of the treatment systems, the environmental impacts of the reactor materials were minimal and the major environmental impact was associated with the operating energy requirements, with each treatment system operating at maximum efficiency. The LCA analysis ignored the CO₂ produced from the oxidation processes, as these contributions were negligible compared to the CO₂ usage from the coal-based electricity used to power the processes. Results of the LCA showed that EAOPs had the lowest environmental impacts of the three processes with regard to CO₂ production and human health impacts, which were both directly a function of energy usage.⁸⁰ The energy needed to remove 1 g L⁻¹ COD was 0.15 kWh for the EAOP, 0.8 kWh for wet air oxidation, and 5.0 kWh for UV/TiO₂. The energy needed to remove 1 g L⁻¹ total phenol was 1.2 kWh for the EAOP, 2.9 kWh for wet air oxidation, and 14.2 kWh for UV/TiO₂. The energy consumption mapped linearly with kg CO₂ equivalents produced, and thus the removal of 1 g L⁻¹ COD resulted in 0.16 kg CO₂ equivalents for EAOP, 0.88 kg CO₂ equivalents for wet air oxidation, and 5.2 kg CO₂ equivalents for UV/TiO₂. Likewise, the removal of 1 g/L phenol resulted in 1.24 kg CO₂ equivalents for EAOP, 3.0 kg CO₂ equivalents for wet air oxidation, and 14.63 kg CO₂ equivalents for UV/TiO₂. Trends in the human health LCA indicator also mirrored the results found for energy consumption,⁸⁰ and therefore, based on this analysis the use of clean and renewable energy sources would greatly lower the environmental impact of the analyzed AOPs. The much higher energy requirements found for UV/TiO₂ in the Chatzisyemon et al.⁸⁰ study was consistent with previous reports that concluded that UV-based AOPs require much more energy than non-UV AOPs.⁷⁹ The work by Chatzisyemon et al.⁸⁰ is a good starting point for LCA analyses of EAOPs, however, more LCA work is needed that evaluates toxic byproduct formation that results from various EAOPs and AOPs to fully assess their environmental impacts.

III. Future Research Needs

Based on the review of the literature, future research in the area of EAOPs should be directed towards 1) improving the understanding of the fundamental science of EAOPs, 2) advancing the development of EAOP technologies to facilitate their implementation in applied

settings, and 3) determining the implications of applying EAOP technologies for water treatment from both an economic and environmental perspective.

A. Fundamental Science of EAOPs

There is a large body of knowledge on the effectiveness of EAOP electrodes for oxidation of a wide variety of compounds across several chemical classes. However, fewer studies were dedicated to understanding the mechanisms of compound transformation at the electrode surface. Future experimental work should seek to gain mechanistic information that can be complemented by *in situ* spectroscopic techniques (e.g., ATR-FTIR, electrochemical impedance spectroscopy (EIS)) and DFT simulations. These types of studies will allow for an understanding of the mechanisms responsible for compound transformations and thus allow a better design of the electrochemical reactors and operating conditions. Additional physical and electrochemical characterization of EAOP electrodes is needed in order to develop structure-function relationships for the oxidation of important classes of contaminants. Advanced scanning electrochemical microscopy techniques are able to spatially map the electrochemical responsiveness of electrodes on the micron-scale, and this information is valuable in tailoring the reactivity of electrode materials.³⁰⁹ However, only few studies have employed this powerful technique for the understanding of EAOP electrodes.^{192,193} Additionally, research should focus on the development of new EAOP electrodes that are inexpensive to fabricate and are robust during operation. Fundamental research is also needed on the further development of porous electrodes and electrodes that limit toxic byproduct formation in order to overcome the inherent limitations of EAOPs.

B. Facilitating EAOP Technology Application

Key challenges remain before EAOPs can be widely implemented for water treatment. Primary challenges include the formation of ClO_4^- and HOC byproducts during oxidation of waste streams, and the low electro-active surface area of electrode materials. Preventing ClO_4^- formation is especially important because it is a terminal product of Cl^- oxidation, and the presence of Cl^- is ubiquitous in waste streams and natural waters. Furthermore, ClO_4^- is not easily reduced back to Cl^- by either chemical or electrochemical processes.³¹⁰⁻³¹⁴ Current research suggests that operational strategies can limit ClO_4^- formation,^{27,315} and thus future research directed at further optimizing operational strategies is necessary.

The relatively low electroactive surface area for electrode materials has also hindered wide spread adoption of EAOPs. The low surface area of parallel plate electrodes results in slow conversion rates of contaminants due to mass transport limitation or otherwise increases the overall electrochemical cells needed to treat a given volume of water. Large numbers of electrochemical cells translates to high capital costs, and prevents adoption of the relatively new EAOP technology. The surge in activity in development of advanced electrode and catalytic materials (e.g., nanofiber and microporous monolithic electrodes) in a number of fields, should be utilized for EAOPs. Operating strategies to incorporate these materials in flow-through mode opposed to flow-by mode electrochemical cells should also be a key focus of future work.

Additionally, applied research on the appropriate pretreatment and post-treatment technologies necessary for implementation of EAOPs should be identified. These pretreatment and post-treatment processes will undoubtedly be linked to the specific water treatment application. The identification of niche applications for EAOPs or

the incorporation of them into hybrid treatment systems should also be explored.

C. Economics and Environmental Impacts of EAOPs

Studies are needed that focus on identifying and quantifying the various environmental impacts of EAOPs and minimizing the cost of EAOP operation. Limited studies exist on these important topics, and this information is crucial to engineers and decision makers in charge of adapting new technologies. Future work should focus on increasing the complexity of LCA models, so that the full environmental sustainability of EAOPs and competing technologies can be assessed. More studies are also needed that provide a full cost analysis of EAOPs for specific water treatment scenarios and optimization work is needed to decrease the operating cost of these technologies. Additionally, the possibility of energy recovery from cathodic reactions (e.g., H_2 production and CO_2 reduction) working in parallel with EAOPs should be addressed from both a technical and economic perspective. Determining the cost and environmental impacts of EAOPs are imperative in identifying appropriate applications for this new technology.

Acknowledgements

I thank the University of Illinois at Chicago for funding to complete this work.

References

1. G. V. Buxton, C. L. Greenstock, W. P. Helman and A. B. Ross, *J. Phys. Chem. Ref. Data*, 1988, **17**, 513-886.
2. C. Comninellis and C. Pulgarin, *Journal of Applied Electrochemistry*, 1993, **23**, 108-112.
3. C. Borrás, C. Berzoy, J. Mostany and B. Scharifker, *Journal of Applied Electrochemistry*, 2006, **36**, 433-439.
4. B. Adams, M. Tian and A. Chen, *Electrochimica Acta*, 2009, **54**, 1491-1498.
5. Q. Zhuo, S. Deng, B. Yang, J. Huang and G. Yu, *Environmental Science & Technology*, 2011, **45**, 2973-2979.
6. H. Sharifian and D. W. Kirk, *Journal of the Electrochemical Society*, 1986, **133**, 921-924.
7. C. Borrás, T. Laredo, J. Mostany and B. R. Scharifker, *Electrochimica Acta*, 2004, **49**, 641-648.
8. C. Borrás, T. Laredo and B. R. Scharifker, *Electrochimica Acta*, 2003, **48**, 2775-2780.
9. C. Borrás, P. Rodriguez, T. Laredo, J. Mostany and B. R. Scharifker, *Journal of Applied Electrochemistry*, 2004, **34**, 583-589.
10. Y. Liu, H. Liu and Y. Li, *Applied Catalysis B-Environmental*, 2008, **84**, 297-302.
11. G. H. Zhao, Y. G. Zhang, Y. Z. Lei, B. Y. Lv, J. X. Gao, Y. A. Zhang and D. M. Li, *Environmental Science & Technology*, 2010, **44**, 1754-1759.
12. J. Iniesta, P. A. Michaud, M. Panizza, G. Cerisola, A. Aldaz and C. Comninellis, *Electrochim. Acta*, 2001, **46**, 3573-3578.

13. P. A. Michaud, M. Panizza, L. Ouattara, T. Diaco, G. Foti and C. Comninellis, *Journal of Applied Electrochemistry*, 2003, **33**, 151-154.
14. J. F. Zhi, H. B. Wang, T. Nakashima, T. N. Rao and A. Fujishima, *J. Phys. Chem. B*, 2003, **107**, 13389-13395.
15. P. Canizares, J. Lobato, R. Paz, M. A. Rodrigo and C. Saez, *Water Research*, 2005, **39**, 2687-2703.
16. K. E. Carter and J. Farrell, *Environmental Science & Technology*, 2008, **42**, 6111-6115.
17. J. M. Kesselman, O. Weres, N. S. Lewis and M. R. Hoffmann, *Journal of Physical Chemistry B*, 1997, **101**, 2637-2643.
18. D. Bejan, J. D. Malcolm, L. Morrison and N. J. Bunce, *Electrochimica Acta*, 2009, **54**, 5548-5556.
19. D. Bejan, E. Guinea and N. J. Bunce, *Electrochimica Acta*, 2012, **69**, 275-281.
20. A. M. Zaky and B. P. Chaplin, *Environmental Science & Technology*, 2013, **47**, 6554-6563.
21. C. Comninellis, *Electrochimica Acta*, 1994, **39**, 1857-1862.
22. D. Pavlov and B. Monahov, *Journal of the Electrochemical Society*, 1996, **143**, 3616-3629.
23. B. Marselli, J. Garcia-Gomez, P. A. Michaud, M. A. Rodrigo and C. Comninellis, *Journal of the Electrochemical Society*, 2003, **150**, D79-D83.
24. X. P. Zhu, M. P. Tong, S. Y. Shi, H. Z. Zhao and J. R. Ni, *Environmental Science & Technology*, 2008, **42**, 4914-4920.
25. A. Kapalka, G. Foti and C. Comninellis, *Electrochimica Acta*, 2009, **54**, 2018-2023.
26. C. Flox, C. Arias, E. Brillas, A. Savall and K. Groenen-Serrano, *Chemosphere*, 2009, **74**, 1340-1347.
27. A. Donaghue and B. P. Chaplin, *Environmental science & technology*, 2013, **47**, 12391-12399.
28. B. P. Chaplin, G. Schrader and J. Farrell, *Environmental Science & Technology*, 2009, **43**, 8302-8307.
29. B. P. Chaplin, G. Schrader and J. Farrell, *Environmental Science & Technology*, 2010, **44**, 4264-4269.
30. L. Gherardini, P. A. Michaud, M. Panizza and C. Comninellis, *J. Electrochem. Soc.*, 2001, **148**, D78-D82.
31. P. L. Hagans, P. M. Natishan, B. R. Stoner and W. E. O'Grady, *J. Electrochem. Soc.*, 2001, **148**, E298-E301.
32. X. P. Zhu, S. Y. Shi, J. J. Wei, F. X. Lv, H. Z. Zhao, J. T. Kong, Q. He and J. R. Ni, *Environmental Science & Technology*, 2007, **41**, 6541-6546.
33. C. Borrás, C. Berzoy, J. Mostany, J. C. Herrera and B. R. Scharifker, *Applied Catalysis B-Environmental*, 2007, **72**, 98-104.
34. P. Canizares, J. Garcia-Gomez, C. Saez and M. A. Rodrigo, *Journal of Applied Electrochemistry*, 2003, **33**, 917-927.
35. P. Canizares, J. Lobato, J. Garcia-Gomez and M. A. Rodrigo, *Journal of Applied Electrochemistry*, 2004, **34**, 111-117.
36. X. M. Chen, F. R. Gao and G. H. Chen, *Journal of Applied Electrochemistry*, 2005, **35**, 185-191.
37. T. A. Enache and A. M. Oliveira-Brett, *Journal of Electroanalytical Chemistry*, 2011, **655**, 9-16.
38. C. Y. Gao and M. Chang, *Acta Physico-Chimica Sinica*, 2008, **24**, 1988-1994.
39. Z. Liao and J. Farrell, *Journal of Applied Electrochemistry*, 2009, **39**, 1993-1999.
40. J. Niu, H. Lin, J. Xu, H. Wu and Y. Li, *Environmental Science & Technology*, 2012, **46**, 10191-10198.
41. T. Ochiai, Y. Iizuka, K. Nakata, T. Murakami, D. A. Tryk, A. Fujishima, Y. Koide and Y. Morito, *Diamond and Related Materials*, 2011, **20**, 64-67.
42. J. Niu, H. Lin, G. Chen and Z. Sun, *Environ Sci Technol*, 2013, [dx.doi.org/10.1021/es402987t](https://doi.org/10.1021/es402987t).
43. K. E. Carter and J. Farrell, *Environmental Science & Technology*, 2009, **43**, 8350-8354.
44. K. Van Hege, M. Verhaege and W. Verstraete, *Water Research*, 2004, **38**, 1550-1558.
45. A. Y. Bagastyo, D. J. Batstone, I. Kristiana, W. Gernjak, C. Joll and J. Radjenovic, *Water Research*, 2012, **46**, 6104-6112.
46. A. Y. Bagastyo, D. J. Batstone, K. Rabaey and J. Radjenovic, *Water Research*, 2013, **47**, 242-250.
47. E. Dialynas, D. Mantzavinos and E. Diamadopoulos, *Water Research*, 2008, **42**, 4603-4608.
48. G. Perez, A. R. Fernandez-Alba, A. M. Urriaga and I. Ortiz, *Water Research*, 2010, **44**, 2763-2772.
49. A. Anglada, D. Ortiz, A. M. Urriaga and I. Ortiz, *Water Science and Technology*, 2010, **61**, 2211-2217.
50. A. Anglada, A. Urriaga and I. Ortiz, *Environmental Science & Technology*, 2009, **43**, 2035-2040.
51. A. Anglada, A. Urriaga, I. Ortiz, D. Mantzavinos and E. Diamadopoulos, *Water Research*, 2011, **45**, 828-838.
52. A. Anglada, A. M. Urriaga and I. Ortiz, *Journal of Hazardous Materials*, 2010, **181**, 729-735.
53. A. Cabeza, A. Urriaga, M.-J. Rivero and I. Ortiz, *Journal of Hazardous Materials*, 2007, **144**, 715-719.
54. A. Cabeza, A. M. Urriaga and I. Ortiz, *Industrial & Engineering Chemistry Research*, 2007, **46**, 1439-1446.
55. L. C. Chiang, J. E. Chang and C. T. Chung, *Environmental Engineering Science*, 2001, **18**, 369-379.
56. G. Perez, J. Saiz, R. Ibanez, A. M. Urriaga and I. Ortiz, *Water Research*, 2012, **46**, 2579-2590.
57. N. N. Rao, M. Rohit, G. Nitin, P. N. Parameswaran and J. K. Astik, *Chemosphere*, 2009, **76**, 1206-1212.
58. M. J. Martin de Vidales, J. Robles-Molina, J. C. Dominguez-Romero, P. Canizares, C. Saez, A. Molina-

- Diaz and M. A. Rodrigo, *J. Chem. Technol. Biotechnol.*, 2012, **87**, 1441-1449.
59. J. R. Dominguez, T. Gonzalez, P. Palo and J. Sanchez-Martin, *Industrial & Engineering Chemistry Research*, 2010, **49**, 8353-8359.
60. J. R. Dominguez, T. Gonzalez, P. Palo, J. Sanchez-Martin, M. A. Rodrigo and C. Saez, *Water Air and Soil Pollution*, 2012, **223**, 2685-2694.
61. L. Feng, E. D. van Hullebusch, M. A. Rodrigo, G. Esposito and M. A. Oturan, *Chemical Engineering Journal*, 2013, **228**, 944-964.
62. M. Muruganathan, S. Yoshihara, T. Rakuma, N. Uehara and T. Shirakashi, *Electrochimica Acta*, 2007, **52**, 3242-3249.
63. M. Muruganathan, S. Yoshihara, T. Rakuma and T. Shirakashi, *Journal of Hazardous Materials*, 2008, **154**, 213-220.
64. C. L. K. Tennakoon, R. C. Bhardwaj and J. O. Bockris, *Journal of Applied Electrochemistry*, 1996, **26**, 18-29.
65. A. Savall, *Chimia*, 1995, **49**, 23-27.
66. K. Juttner, U. Galla and H. Schmieder, *Electrochimica Acta*, 2000, **45**, 2575-2594.
67. D. Rajkumar and K. Palanivelu, *Journal of Hazardous Materials*, 2004, **113**, 123-129.
68. L. Ouattara, M. M. Chowdhry and C. Comninellis, *New Diamond and Frontier Carbon Technology*, 2004, **14**, 239-247.
69. S. S. Vaghela, A. D. Jethva, B. B. Mehta, S. P. Dave, S. Adimurthy and G. Ramachandraiah, *Environmental Science & Technology*, 2005, **39**, 2848-2855.
70. P. Canizares, R. Paz, J. Lobato, C. Saez and M. A. Rodrigo, *Journal of Hazardous Materials*, 2006, **138**, 173-181.
71. E. Chatzisymeon, N. P. Xekoukoulotakis, A. Coz, N. Kalogerakis and D. Mantzavinos, *Journal of Hazardous Materials*, 2006, **137**, 998-1007.
72. N. Mohan, N. Balasubramanian and C. A. Basha, *Journal of Hazardous Materials*, 2007, **147**, 644-651.
73. V. K. Gupta, R. Jain and S. Varshney, *Journal of Colloid and Interface Science*, 2007, **312**, 292-296.
74. S. Masid, S. Waghmare, N. Gedam, R. Misra, R. Dhodapkar, T. Nandy and N. N. Rao, *Desalination*, 2010, **259**, 192-196.
75. H. Suty, C. De Traversay and M. Cost, *Water Science and Technology*, 2004, **49**, 227-233.
76. J. J. Pignatello, E. Oliveros and A. MacKay, *Crit. Rev. Environ. Sci. Technol.*, 2006, **36**, 1-84.
77. K. Ikehata, N. J. Naghashkar and M. G. Ei-Din, *Ozone-Science & Engineering*, 2006, **28**, 353-414.
78. C. Comninellis, A. Kapalka, S. Malato, S. A. Parsons, L. Poullos and D. Mantzavinos, *J. Chem. Technol. Biotechnol.*, 2008, **83**, 769-776.
- M. N. Chong, A. K. Sharma, S. Burn and C. P. Saint, *Journal of Cleaner Production*, 2012, **35**, 230-238.
80. E. Chatzisymeon, S. Foteinis, D. Mantzavinos and T. Tsoutsos, *Journal of Cleaner Production*, 2013, **54**, 229-234.
81. A. Matilainen and M. Sillanpaa, *Chemosphere*, 2010, **80**, 351-365.
82. B. I. Escher and K. Fenner, *Environmental Science & Technology*, 2011, **45**, 3835-3847.
83. I. Oller, S. Malato and J. A. Sanchez-Perez, *Science of the Total Environment*, 2011, **409**, 4141-4166.
84. J. Jiang, M. Chang and P. Pan, *Environ. Sci. Technol.*, 2008.
85. P. Canizares, R. Paz, C. Saez and M. A. Rodrigo, *Journal of Environmental Management*, 2009, **90**, 410-420.
86. E. Brillas, I. Sires and M. A. Oturan, *Chemical Reviews*, 2009, **109**, 6570-6631.
87. M. Umar, H. A. Aziz and M. S. Yusoff, *Waste Management*, 2010, **30**, 2113-2121.
88. P. V. Nidheesh and R. Gandhimathi, *Desalination*, 2012, **299**, 1-15.
89. E. Rosales, M. Pazos and M. A. Sanroman, *Chemical Engineering & Technology*, 2012, **35**, 609-617.
90. A. Yaqub and H. Ajab, *Reviews in Chemical Engineering*, 2013, **29**, 123-130.
91. K. Rajeshwar, J. G. Ibanez and G. M. Swain, *Journal of Applied Electrochemistry*, 1994, **24**, 1077-1091.
92. T. Ochiai and A. Fujishima, *Journal of Photochemistry and Photobiology C-Photochemistry Reviews*, 2012, **13**, 247-262.
93. G. H. Chen, *Separation and Purification Technology*, 2004, **38**, 11-41.
94. M. Panizza and G. Cerisola, *Electrochimica Acta*, 2005, **51**, 191-199.
95. C. A. Martinez-Huitle and S. Ferro, *Chemical Society Reviews*, 2006, **35**, 1324-1340.
96. A. Kraft, *International Journal of Electrochemical Science*, 2007, **2**, 355-385.
97. M. Panizza and G. Cerisola, *Chemical Reviews*, 2009, **109**, 6541-6569.
98. C. A. Martinez-Huitle and E. Brillas, *Applied Catalysis B-Environmental*, 2009, **87**, 105-145.
99. C. A. Martinez-Huitle and L. S. Andrade, *Quimica Nova*, 2011, **34**, 850-858.
100. M. H. P. Santana, L. A. De Faria and J. F. C. Boodts, *Electrochimica Acta*, 2005, **50**, 2017-2027.
101. S. Fierro, T. Nagel, H. Baltruschat and C. Comninellis, *Electrochemistry Communications*, 2007, **9**, 1969-1974.
102. C. Comninellis and A. DeBattisti, *Journal De Chimie Physique Et De Physico-Chimie Biologique*, 1996, **93**, 673-679.

103. O. Simond, V. Schaller and C. Comninellis, *Electrochimica Acta*, 1997, **42**, 2009-2012.
104. G. Foti, D. Gandini, C. Comninellis, A. Perret and W. Haenni, *Electrochemical and Solid State Letters*, 1999, **2**, 228-230.
105. USEPA National Primary Drinking Water Regulations Home Page.
<http://water.epa.gov/drink/contaminants/index.cfm>.
106. Y. S. Hsu and S. K. Ghandhi, *Journal of the Electrochemical Society*, 1980, **127**, 1592-1595.
107. Y. S. Hsu and S. K. Ghandhi, *Journal of the Electrochemical Society*, 1980, **127**, 1595-1599.
108. R. Kotz, S. Stucki and B. Carcer, *Journal of Applied Electrochemistry*, 1991, **21**, 14-20.
109. H. Liu, A. Vajpayee and C. D. Vecitis, *Acs Applied Materials & Interfaces*, 2013, **5**, 10054-10066.
110. S. Stucki, R. Kotz, B. Carcer and W. Suter, *Journal of Applied Electrochemistry*, 1991, **21**, 99-104.
111. C. Pulgarin, N. Adler, P. Peringer and C. Comninellis, *Water Research*, 1994, **28**, 887-893.
112. R. Cossu, A. M. Polcaro, M. C. Lavagnolo, M. Mascia, S. Palmas and F. Renoldi, *Environmental Science & Technology*, 1998, **32**, 3570-3573.
113. J. H. Grimm, D. G. Bessarabov, U. Simon and R. D. Sanderson, *Journal of Applied Electrochemistry*, 2000, **30**, 293-302.
114. S. Tanaka, Y. Nakata, T. Kimura, Yustiawati, M. Kawasaki and H. Kuramitz, *Journal of Applied Electrochemistry*, 2002, **32**, 197-201.
115. C. Zanta, P. A. Michaud, C. Comninellis, A. R. De Andrade and J. F. C. Boodts, *Journal of Applied Electrochemistry*, 2003, **33**, 1211-1215.
116. M. Quiroz, S. Reyna and J. Sanchez, *Journal of Solid State Electrochemistry*, 2003, **7**, 277-282.
117. X. M. Chen and G. H. Chen, *Electrochimica Acta*, 2005, **50**, 4155-4159.
118. Y. H. Wang, K. Y. Chan, X. Y. Li and S. K. So, *Chemosphere*, 2006, **65**, 1087-1093.
119. L. Lipp and D. Pletcher, *Electrochimica Acta*, 1997, **42**, 1091-1099.
120. B. CorreaLozano, C. Comninellis and A. DeBattisti, *Journal of Applied Electrochemistry*, 1997, **27**, 970-974.
121. F. Montilla, E. Morallon and J. L. Vazquez, *Journal of the Electrochemical Society*, 2005, **152**, B421-B427.
122. F. Montilla, E. Morallon, A. De Battisti, S. Barison, S. Daolio and J. L. Vazquez, *Journal of Physical Chemistry B*, 2004, **108**, 15976-15981.
123. F. Montilla, E. Morallon, A. De Battisti and J. L. Vazquez, *Journal of Physical Chemistry B*, 2004, **108**, 5036-5043.
124. G. Li, Y. H. Wang and Q. Y. Chen, *Journal of Solid State Electrochemistry*, 2013, **17**, 1303-1309.
125. S. Ferro, C. A. Martinez-Huitle and A. De Battisti, *Journal of Applied Electrochemistry*, 2010, **40**, 1779-1787.
126. D. V. Smith and A. P. Watkinson, *Can. J. Chem. Eng. J.*, 1981, **59**, 52-59.
127. N. B. Tahar, R. Abdelhedi and A. Savall, *Journal of Applied Electrochemistry*, 2009, **39**, 663-669.
128. N. B. Tahar and A. Savall, *Journal of the Electrochemical Society*, 1998, **145**, 3427-3434.
129. N. B. Tahar and A. Savall, *Journal of New Materials for Electrochemical Systems*, 1999, **2**, 19-26.
130. N. B. Tahar and A. Savall, *Journal of Applied Electrochemistry*, 1999, **29**, 277-283.
131. M. Panizza and G. Cerisola, *Industrial & Engineering Chemistry Research*, 2008, **47**, 6816-6820.
132. L. L. Houk, S. K. Johnson, J. Feng, R. S. Houk and D. C. Johnson, *Journal of Applied Electrochemistry*, 1998, **28**, 1167-1177.
133. F. Bonfatti, S. Ferro, F. Lavezzo, M. Malacarne, G. Lodi and A. De Battisti, *Journal of the Electrochemical Society*, 1999, **146**, 2175-2179.
134. A. H. Ras and J. F. van Staden, *Journal of Applied Electrochemistry*, 1999, **29**, 313-319.
135. Y. Song, G. Wei and R. Xiong, *Electrochimica Acta*, 2007, **52**, 7022-7027.
136. C. A. Martinez-Huitle, M. A. Quiroz, C. Comninellis, S. Ferro and A. De Battisti, *Electrochimica Acta*, 2004, **50**, 949-956.
137. D. Wu, M. Liu, D. Dong and X. Zhou, *Microchemical Journal*, 2007, **85**, 250-256.
138. Y. Cong and Z. Wu, *Journal of Physical Chemistry C*, 2007, **111**, 3442-3446.
139. D. Pavlov, *Journal of the Electrochemical Society*, 1992, **139**, 3075-3080.
140. H. Liu, Y. Liu, C. Zhang and R. Shen, *Journal of Applied Electrochemistry*, 2008, **38**, 101-108.
141. S. Abaci, U. Tamer, K. Pekmez and A. Yildiz, *Applied Surface Science*, 2005, **240**, 112-119.
142. I. Sires, C. T. J. Low, C. Ponce-de-Leon and F. C. Walsh, *Electrochimica Acta*, 2010, **55**, 2163-2172.
143. P. C. S. Hayfield, Royal Society of Chemistry: Cambridge, UK, 2002.
144. G. Y. Chen, C. C. Waraksa, H. G. Cho, D. D. Macdonald and T. E. Mallouk, *Journal of the Electrochemical Society*, 2003, **150**, E423-E428.
145. F. C. Walsh and R. G. A. Wills, *Electrochimica Acta*, 2010, **55**, 6342-6351.
146. G. Chen, E. A. Betterton, R. G. Arnold and W. P. Ela, *Journal of Applied Electrochemistry*, 2003, **33**, 161-169.
147. D. Bejan, L. M. Rabson and N. J. Bunce, *Canadian Journal of Chemical Engineering*, 2007, **85**, 929-935.

148. J. R. Smith, F. C. Walsh and R. L. Clarke, *Journal of Applied Electrochemistry*, 1998, **28**, 1021-1033.
149. G. Chen, S. R. Bare and T. E. Mallouk, *J. Electrochem. Soc.*, 2002, **149**, A1092-A1099.
150. G. Chen, E. A. Betterton and R. G. Arnold, *J. Appl. Electrochem.*, 1999, **29**, 961-970.
151. K. Ellis, A. Hill, J. Hill, A. Loyns and T. Partington, *Journal of Power Sources*, 2004, **136**, 366-371.
152. T. Ioroi, H. Senoh, S.-I. Yamazaki, Z. Siroma, N. Fujiwara and K. Yasuda, *Journal of the Electrochemical Society*, 2008, **155**, B321-B326.
153. G. Y. Chen, S. R. Bare and T. E. Mallouk, *Journal of the Electrochemical Society*, 2002, **149**, A1092-A1099.
154. S. El-Sherif, D. Bejan and N. J. Bunce, *Canadian Journal of Chemistry-Revue Canadienne De Chimie*, 2010, **88**, 928-936.
155. C. Schwandt and D. J. Fray, *Electrochimica Acta*, 2005, **51**, 66-76.
156. D. Morris, Y. Dou, J. Rebane, C. E. J. Mitchell, R. G. Egdell, D. S. L. Law, A. Vittadini and M. Casarin, *Physical Review B*, 2000, **61**, 13445.
157. R. D. Shannon, *Acta Crystallographica Section A*, 1976, **32**, 751-767.
158. H. Chhina, S. Campbell and O. Kesler, *Journal of the Electrochemical Society*, 2009, **156**, B1232-B1237.
159. A. Bauer, L. Chevallier, R. Hui, S. Cavaliere, J. Zhang, D. Jones and J. Roziere, *Electrochimica Acta*, 2012, **77**, 1-7.
160. M. Fehse, S. Cavaliere, P. E. Lippens, I. Savych, A. Iadecola, L. Monconduit, D. J. Jones, J. Roziere, F. Fischer, C. Tessier and L. Stievanot, *Journal of Physical Chemistry C*, 2013, **117**, 13827-13835.
161. P. Hasin, M. A. Alpuche-Aviles, Y. G. Li and Y. Y. Wu, *Journal of Physical Chemistry C*, 2009, **113**, 7456-7460.
162. S. Lee, J. H. Noh, H. S. Han, D. K. Yim, D. H. Kim, J.-K. Lee, J. Y. Kim, H. S. Jung and K. S. Hong, *Journal of Physical Chemistry C*, 2009, **113**, 6878-6882.
163. M. Yang, D. Kim, H. Jha, K. Lee, J. Paul and P. Schmuki, *Chemical Communications*, 2011, **47**, 2032-2034.
164. S. G. Kim, M. J. Ju, I. T. Choi, W. S. Choi, H.-J. Choi, J.-B. Baek and H. K. Kim, *Rsc Advances*, 2013, **3**, 16380-16386.
165. C. Das, P. Roy, M. Yang, H. Jha and P. Schmuki, *Nanoscale*, 2011, **3**, 3094-3096.
166. M. Z. Atashbar, H. T. Sun, B. Gong, W. Wlodarski and R. Lamb, *Thin Solid Films*, 1998, **326**, 238-244.
167. A. M. Ruiz, A. Cornet, K. Shimanoe, J. R. Morante and N. Yamazoe, *Sensors and Actuators B: Chemical*, 2005, **108**, 34-40.
168. M. Garcia-Mota, A. Vojvodic, H. Metiu, I. C. Man, H.-Y. Su, J. Rossmeisl and J. K. Nørskov, *Chemcatchem*, 2011, **3**, 1607-1611.
169. W. Haenni, P. Rychen, M. Fryda and C. Comminellis, in *Thin-Film Diamond II*, 2004, vol. 77, pp. 149-196.
170. J. Ristein, *Science*, 2006, **313**, 1057-1058.
171. A. Kraft, *Int. J. Electrochem. Sci.*, 2007, **2**, 355 - 385.
172. J. Xu, M. C. Granger, Q. Chen, J. W. Strojek, T. E. Lister and G. M. Swain, *Anal. Chem.*, 1997, **69**, 591A-597A.
173. G. M. Swain and R. Ramesham, *Analytical Chemistry*, 1993, **65**, 345-351.
174. J. S. Xu, M. C. Granger, Q. Y. Chen, J. W. Strojek, T. E. Lister and G. M. Swain, *Analytical Chemistry*, 1997, **69**, A591-A597.
175. D. Gandini, P. A. Michaud, I. Duo, E. Mahe, W. Haenni, A. Perret and C. Comminellis, *New Diamond and Frontier Carbon Technology*, 1999, **9**, 303-316.
176. Y. Show, M. A. Witek, P. Sonthalia and G. M. Swain, *Chemistry of Materials*, 2003, **15**, 879-888.
177. A. Ay, V. M. Swope and G. M. Swain, *Journal of the Electrochemical Society*, 2008, **155**, B1013-B1022.
178. S. Wang, V. M. Swope, J. E. Bulter, T. Feygelson and G. M. Swain, *Diamond and Related Materials*, 2009, **18**, 669-677.
179. A. F. Azevedo, N. A. Braga, F. A. Souza, J. T. Matsushima, M. R. Baldan and N. G. Ferreira, *Diamond and Related Materials*, 2010, **19**, 462-465.
180. B. P. Chaplin, I. Wylie, H. Zheng, J. A. Carlisle and J. Farrell, *J. Appl. Electrochem.*, 2011, **41**, 1329-1340.
181. B. P. Chaplin, D. K. Hubler and J. Farrell, *Electrochimica Acta*, 2013, **89**, 122-131.
182. A. E. Fischer, Y. Show and G. M. Swain, *Analytical Chemistry*, 2004, **76**, 2553-2560.
183. M. Fryda, D. Herrmann, L. Schafer, C. P. Klages, A. Perret, W. Haenni, C. Comminellis and D. Gandini, *New Diamond and Frontier Carbon Technology*, 1999, **9**, 229-240.
184. Y. Xin, F. Liu, J. Wang and X. Li, *Rare Metal Materials and Engineering*, 2012, **41**, 247-249.
185. I. Gerger, R. Haubner, H. Kronberger and G. Fafilek, *Diamond and Related Materials*, 2004, **13**, 1062-1069.
186. V. Fisher, D. Gandini, S. Laufer, E. Blank and C. Comminellis, *Electrochimica Acta*, 1998, **44**, 521-524.
187. Y. Tian, X. M. Chen, C. Shang and G. H. Chen, *Journal of the Electrochemical Society*, 2006, **153**, J80-J85.
188. W. M. Haynes, *CRC Handbook of Chemistry and Physics, 91st Edition*, CRC Press, New York, 2010.
189. P. Y. Lim, F. Y. Lin, H. C. Shih, V. G. Ralchenko, V. P. Varnin, Y. V. Pleskov, S. F. Hsu, S. S. Chou and P. L. Hsu, *Thin Solid Films*, 2008, **516**, 6125-6132.
190. M. A. Lowe, A. E. Fischer and G. M. Swain, *Journal of the Electrochemical Society*, 2006, **153**, B506-B511.
191. T. Kolber, K. Piplits, R. Haubner and H. Hutter, *Fresenius' J. Anal. Chem.*, 1999, **365**, 636-641.

192. K. B. Holt, A. J. Bard, Y. Show and G. M. Swain, *J. Phys. Chem. B*, 2004, **108**, 15117-15127.
193. H. V. Patten, S. C. S. Lai, J. V. Macpherson and P. R. Unwin, *Analytical Chemistry*, 2012, **84**, 5427-5432.
194. H. B. Martin, A. Argoitia, J. C. Angus and U. Landau, *Journal of the Electrochemical Society*, 1999, **146**, 2959-2964.
195. C. H. Goeting, F. Marken, A. Gutierrez-Sosa, R. G. Compton and J. S. Foord, *Diamond and Related Materials*, 2000, **9**, 390-396.
196. H. Girard, N. Simon, D. Ballutaud, M. Herlern and A. Etcheberry, *Diamond and Related Materials*, 2007, **16**, 316-325.
197. N. Simon, H. Girard, D. Ballutaud, S. Ghodbane, A. Deneuille, M. Herlem and A. Etcheberry, *Diamond and Related Materials*, 2005, **14**, 1179-1182.
198. M. Wang, N. Simon, G. Charrier, M. Bouttemy, A. Etcheberry, M. S. Li, R. Boukherroub and S. Szunerits, *Electrochemistry Communications*, 2010, **12**, 351-354.
199. M. Wang, N. Simon, C. Decorse-Pascanut, M. Bouttemy, A. Etcheberry, M. S. Li, R. Boukherroub and S. Szunerits, *Electrochimica Acta*, 2009, **54**, 5818-5824.
200. O. Azizi, D. Hubler, G. Schrader, J. Farrell and B. P. Chaplin, *Environ. Sci. Technol.*, 2011, **45**, 10582-10590.
201. I. Yagi, H. Notsu, T. Kondo, D. A. Tryk and A. Fujishima, *J. Electroanal. Chem.*, 1999, **473**, 173-178.
202. M. C. Granger and G. M. Swain, *Journal of the Electrochemical Society*, 1999, **146**, 4551-4558.
203. D. Mishra, Z. H. Liao and J. Farrell, *Environmental Science & Technology*, 2008, **42**, 9344-9349.
204. B. J. Hwang and K. L. Lee, *Journal of Applied Electrochemistry*, 1996, **26**, 153-159.
205. A. M. Polcaro and S. Palmas, *Industrial & Engineering Chemistry Research*, 1997, **36**, 1791-1798.
206. A. M. Polcaro, S. Palmas, F. Renoldi and M. Mascia, *Journal of Applied Electrochemistry*, 1999, **29**, 147-151.
207. J. D. Rodgers, W. Jedral and N. I. Bunce, *Environmental Science & Technology*, 1999, **33**, 1453-1457.
208. M. A. Rodrigo, P. A. Michaud, I. Duo, M. Panizza, G. Cerisola and C. Comninellis, *Journal of the Electrochemical Society*, 2001, **148**, D60-D64.
209. P. Canizares, F. Martinez, M. Diaz, J. Garcia-Gomez and M. A. Rodrigo, *Journal of the Electrochemical Society*, 2002, **149**, D118-D124.
210. P. Canizares, J. Garcia-Gomez, C. Saez and M. A. Rodrigo, *Journal of Applied Electrochemistry*, 2004, **34**, 87-94.
211. S.-P. Tong, C.-A. Ma and H. Feng, *Electrochimica Acta*, 2008, **53**, 3002-3006.
212. P. Canizares, C. Saez, J. Lobato and M. A. Rodrigo, *Industrial & Engineering Chemistry Research*, 2004, **43**, 1944-1951.
213. P. Canizares, C. Saez, J. Lobato and M. A. Rodrigo, *Electrochimica Acta*, 2004, **49**, 4641-4650.
214. P. Wardman, *Journal of Physical and Chemical Reference Data*, 1989, **18**, 1637-1755.
215. M. Gattrell and D. W. Kirk, *Journal of the Electrochemical Society*, 1992, **139**, 2736-2744.
216. A.-N. Kawde, M. A. Morsy, N. Odewunmi and W. Mahfouz, *Electroanalysis*, 2013, **25**, 1547-1555.
217. Y. Zhang, Q. Li, H. Cui and J. P. Zhai, *Electrochimica Acta*, 2010, **55**, 7219-7224.
218. W. Zhang, L. Y. Bao, X. Y. Zhang, J. He and G. Wei, *Water Environment Research*, 2012, **84**, 2028-2036.
219. C. Terashima, T. N. Rao, B. V. Sarada, D. A. Tryk and A. Fujishima, *Analytical Chemistry*, 2002, **74**, 895-902.
220. C. Flox, E. Brillas, A. Savall and K. Groenen-Serrano, *Current Organic Chemistry*, 2012, **16**, 1960-1966.
221. D. Sopchak, B. Miller, Y. Avyigal and R. Kalish, *Journal of Electroanalytical Chemistry*, 2002, **538**, 39-45.
222. Y. Jiang, X. P. Zhu, H. N. Li and J. R. Ni, *Chemosphere*, 2010, **78**, 1093-1099.
223. N. Rabaaoui and M. S. Allagui, *Journal of Hazardous Materials*, 2012, **243**, 187-192.
224. Y. Zhang, N. Yang, M. Murugananthan and S. Yoshihara, *Journal of Hazardous Materials*, 2013, **244**, 295-302.
225. C. Comninellis and C. Pulgarin, *Journal of Applied Electrochemistry*, 1991, **21**, 703-708.
226. C. A. Martinez-Huitle, S. Ferro and A. De Battisti, *Electrochimica Acta*, 2004, **49**, 4027-4034.
227. M. Tian, S. S. Thind, M. Simko, F. M. Gao and A. C. Chen, *Journal of Physical Chemistry A*, 2012, **116**, 2927-2934.
228. M. C. Tertis, M. Jitaru and L. Silaghi-Dumitrescu, *Revista De Chimie*, 2010, **61**, 360-363.
229. R. Vargas, C. Borrás, D. Plana, J. Mostany and B. R. Scharifker, *Electrochimica Acta*, 2010, **55**, 6501-6506.
230. U. Schumann and P. Grundler, *Water Research*, 1998, **32**, 2835-2842.
231. D. Gandini, E. Mahe, P. A. Michaud, W. Haenni, A. Perret and C. Comninellis, *Journal of Applied Electrochemistry*, 2000, **30**, 1345-1350.
232. K. Scott and H. Cheng, *Journal of Applied Electrochemistry*, 2002, **32**, 583-589.
233. P. Canizares, J. Garcia-Gomez, J. Lobato and M. A. Rodrigo, *Industrial & Engineering Chemistry Research*, 2003, **42**, 956-962.
234. T. A. Ivandini, T. N. Rao, A. Fujishima and Y. Einaga, *Analytical Chemistry*, 2006, **78**, 3467-3471.
235. E. Weiss, K. Groenen-Serrano, A. Savall and C. Comninellis, *Journal of Applied Electrochemistry*, 2007, **37**, 41-47.

236. O. Scialdone, S. Randazzo, A. Galia and G. Silvestri, *Water Research*, 2009, **43**, 2260-2272.
237. A. Kapalka, B. Lanova, H. Baltruschat, G. Foti and C. Comninellis, *Journal of the Electrochemical Society*, 2009, **156**, E149-E153.
238. O. Scialdone, *Electrochimica Acta*, 2009, **54**, 6140-6147.
239. S. Garcia-Segura and E. Brillias, *Water Research*, 2011, **45**, 2975-2984.
240. Y.-H. Huang, Y.-J. Shih and C.-H. Liu, *Journal of Hazardous Materials*, 2011, **188**, 188-192.
241. O. Scialdone, A. Galia and S. Randazzo, *Chemical Engineering Journal*, 2011, **174**, 266-274.
242. O. Scialdone, A. Galia and S. Randazzo, *Chemical Engineering Journal*, 2012, **183**, 124-134.
243. Y.-H. Cui, Y.-J. Feng, J. Liu and N. Ren, *Journal of Hazardous Materials*, 2012, **239**, 225-232.
244. N. Bensalah, B. Louhichi and A. Abdel-Wahab, *International Journal of Environmental Science and Technology*, 2012, **9**, 135-143.
245. P. Canizares, R. Paz, C. Saez and M. A. Rodrigo, *Electrochimica Acta*, 2008, **53**, 2144-2153.
246. R. Andrezzi, V. Caprio, A. Insola, R. Marotta and V. Tufano, *Water Research*, 1998, **32**, 1492-1496.
247. P. C. C. Faria, J. J. M. Orfao and M. F. R. Pereira, *Applied Catalysis B-Environmental*, 2008, **79**, 237-243.
248. H. Ryu, A. Alum and M. Abbaszadegan, *Environmental Science & Technology*, 2005, **39**, 8600-8605.
249. A. Kapalka, B. Lanova, H. Baltruschat, G. Foti and C. Comninellis, *Journal of the Electrochemical Society*, 2008, **155**, E96-E100.
250. A. Kapalka, G. Foti and C. Comninellis, *Journal of the Electrochemical Society*, 2008, **155**, E27-E32.
251. Organization for Economic Co-operation and Development (OECD). Results of survey on production and use of PFOS, PFAS, and PFOA, related substances and products/mixtures containing these substances, Environment Directorate Joint Meeting of the Chemicals Committee and the Working Party on Chemicals, Pesticides and Biotechnology, OECD, Paris, January 13, 2005.
252. S. M. Vyas, I. Kania-Korwel and H. J. Lehmier, *J. Environ. Sci. and Health, Part A*, 2007, **42**, 249-255.
253. K. J. Hansen, L. A. Clemen, M. E. Ellefson and H. O. Johnson, *Environmental Science & Technology*, 2001, **35**, 766-770.
254. S. Taniyasu, K. Kannan, Y. Horii, N. Hanari and N. Yamashita, *Environmental Science & Technology*, 2003, **37**, 2634-2639.
255. M. K. So, S. Taniyasu, N. Yamashita, J. P. Giesy, J. Zheng, Z. Fang, S. H. Im and P. K. S. Lam, *Environmental Science & Technology*, 2004, **38**, 4056-4063.
256. B. Boulanger, A. M. Peck, J. L. Schnoor and K. C. Hornbuckle, *Environmental Science & Technology*, 2005, **39**, 74-79.
257. K. Kannan, S. Corsolini, J. Falandysz, G. Fillmann, K. S. Kumar, B. G. Loganathan, M. A. Mohd, J. Olivero, N. Van Wouwe, J. H. Yang and K. M. Aldous, *Environmental Science & Technology*, 2004, **38**, 4489-4495.
258. K. Kannan, S. Corsolini, J. Falandysz, G. Oehme, S. Focardi and J. P. Giesy, *Environmental Science & Technology*, 2002, **36**, 3210-3216.
259. K. Kannan, J. C. Franson, W. W. Bowerman, K. J. Hansen, J. D. Jones and J. P. Giesy, *Environmental Science & Technology*, 2001, **35**, 3065-3070.
260. K. Kannan, J. Koistinen, K. Beckmen, T. Evans, J. F. Gorzelany, K. J. Hansen, P. D. Jones, E. Helle, M. Nyman and J. P. Giesy, *Environmental Science & Technology*, 2001, **35**, 1593-1598.
261. R. Bossi, F. F. Riget and R. Dietz, *Environmental Science & Technology*, 2005, **39**, 7416-7422.
262. K. J. Hansen, H. O. Johnson, J. S. Eldridge, J. L. Butenhoff and L. A. Dick, *Environmental Science & Technology*, 2002, **36**, 1681-1685.
263. G. W. Olsen, K. J. Hansen, L. A. Stevenson, J. M. Burris and J. H. Mandel, *Environmental Science & Technology*, 2003, **37**, 888-891.
264. K. Inoue, F. Okada, R. Ito, S. Kato, S. Sasaki, S. Nakajima, A. Uno, Y. Saijo, F. Sata, Y. Yoshimura, R. Kishi and H. Nakazawa, *Environmental Health Perspectives*, 2004, **112**, 1204-1207.
265. H. Moriwaki, Y. Takagi, M. Tanaka, K. Tsuruho, K. Okitsu and Y. Maeda, *Environ. Sci. Technol.*, 2005, **39**, 3388-3392.
266. H. F. Schroder and R. J. W. Meesters, Stability of fluorinated surfactants in advanced oxidation processes - A follow up of degradation products using flow injection-mass spectrometry, liquid chromatography-mass spectrometry and liquid chromatography-multiple stage mass spectrometry, 2005.
267. Q. Zhuo, S. Deng, B. Yang, J. Huang, B. Wang, T. Zhang and G. Yu, *Electrochimica Acta*, 2012, **77**, 17-22.
268. H. Lin, J. Niu, S. Ding and L. Zhang, *Water Research*, 2012, **46**, 2281-2289.
269. A. M. Dreizler and E. Roduner, *Fuel Cells*, 2012, **12**, 132-140.
270. A. J. Bard and L. R. Faulkner, *Electrochemical Methods: Fundamentals and Applications*, John Wiley and Sons, 2001.
271. M. Mascia, A. Vacca, S. Palmas and A. M. Polcaro, *Journal of Applied Electrochemistry*, 2007, **37**, 71-76.
272. P. Cañizares, J. García-Gómez, I. Fernández de Marcos, M. A. Rodrigo and J. Lobato, *Journal of Chemical Education*, 2006, **83**, 1204.
273. J. Yang, J. Wang and J. P. Jia, *Environmental Science & Technology*, 2009, **43**, 3796-3802.

274. H. Liu and C. D. Vecitis, *Journal of Physical Chemistry C*, 2012, **116**, 374-383.
275. M. E. Suss, T. F. Baumann, W. L. Bourcier, C. M. Spadaccini, K. A. Rose, J. G. Santiago and M. Stadermann, *Energy & Environmental Science*, 2012, **5**, 9511-9519.
276. P. Westerhoff, G. Aiken, G. Amy and J. Debroux, *Water Research*, 1999, **33**, 2265-2276.
277. B. M. Matthew and C. Anastasio, *Atmospheric Chemistry and Physics*, 2006, **6**, 2423-2437.
278. C. Lee, J. Yoon and U. Von Gunten, *Water Research*, 2007, **41**, 581-590.
279. M. P. Grotheer and E. H. Cook, *Electrochemical Technology*, 1968, **6**, 221-&.
280. N. Munichandraiah and S. Sathyanarayana, *Journal of Applied Electrochemistry*, 1987, **17**, 33-48.
281. N. Munichandraiah and S. Sathyanarayana, *Journal of Applied Electrochemistry*, 1988, **18**, 314-316.
282. N. Munichandraiah and S. Sathyanarayana, *Journal of Applied Electrochemistry*, 1990, **20**, 1059-1062.
283. L. J. J. Janssen and P. D. L. Vanderheyden, *Journal of Applied Electrochemistry*, 1995, **25**, 126-136.
284. M. E. H. Bergmann and J. Rollin, *Catalysis Today*, 2007, **124**, 198-203.
285. M. E. H. Bergmann, J. Rollin and T. Iourtchouk, *Electrochimica Acta*, 2009, **54**, 2102-2107.
286. B. S. Oh, S. G. Oh, Y. Y. Hwang, H.-W. Yu, J.-W. Kang and I. S. Kim, *Science of the Total Environment*, 2010, **408**, 5958-5965.
287. B. S. Oh, S. G. Oh, Y. J. Jung, Y. Y. Hwang, J. W. Kang and I. S. Kim, *Desalination and Water Treatment*, 2010, **18**, 245-250.
288. A. Sanchez-Carretero, C. Saez, P. Canizares and M. A. Rodrigo, *Chemical Engineering Journal*, 2011, **166**, 710-714.
289. J. Boudreau, D. Bejan and N. J. Bunce, *Canadian Journal of Chemistry-Revue Canadienne De Chimie*, 2010, **88**, 418-425.
290. J. Boudreau, D. Bejan, S. Li and N. J. Bunce, *Industrial & Engineering Chemistry Research*, 2010, **49**, 2537-2542.
291. H. Li and J. Ni, *Electrochimica Acta*, 2012, **69**, 268-274.
292. E. T. Urbansky and M. R. Schock, *Journal of Environmental Management*, 1999, **56**, 79-95.
293. E. Urbansky, *Environmental Science and Pollution Research*, 2002, **9**, 187-192.
294. Interim Drinking Water Health Advisory for perchlorate EPA 822-R-08-025; U.S. EPA: Washington, DC, Dec 2008.
295. Perchlorate in drinking water. R-16-04; California Department of Health Services, Sacramento, CA, 2006.
296. Perchlorate fact sheet for public water suppliers; Massachusetts Department of Environmental Protection, Boston, MA, 2006.
297. Y. J. Jung, K. W. Baek, B. S. Oh and J.-W. Kang, *Water Research*, 2010, **44**, 5345-5355.
298. D. Hubler, Ph.D. Dissertation, The University of Arizona. Ann Arbor: ProQuest/UMI. (Publication No. AAT 3548029.), 2012.
299. M. E. H. Bergmann and J. Rollin, *Catalysis Today*, 2007, **124**, 198-203.
300. C. R. Costa, F. Montilla, E. Morallon and P. Olivi, *Electrochimica Acta*, 2009, **54**, 7048-7055.
301. H. Gallard, F. Pellizzari, J. P. Croue and B. Legube, *Water Research*, 2003, **37**, 2883-2892.
302. D. Khamis, E. Mahe, F. Dardoize and D. Devilliers, *Journal of Applied Electrochemistry*, 2010, **40**, 1829-1838.
303. C. Provent, W. Haenni, E. Santoli and P. Rychen, *Electrochimica Acta*, 2004, **49**, 3737-3744.
304. H. N. Li and J. R. Ni, *Electrochimica Acta*, 2012, **69**, 268-274.
305. S. D. Boyce and J. F. Hornig, *Environmental Science & Technology*, 1983, **17**, 202-211.
306. L. M. Rebenne, A. C. Gonzalez and T. M. Olson, *Environmental Science & Technology*, 1996, **30**, 2235-2242.
307. W. A. Arnold, J. Bolotin, U. Von Gunten and T. B. Hofstetter, *Environmental Science & Technology*, 2008, **42**, 7778-7785.
308. D. L. Norwood, R. F. Christman and P. G. Hatcher, *Environmental Science & Technology*, 1987, **21**, 791-798.
309. N. Ebejer, A. G. Guell, S. C. S. Lai, K. McKelvey, M. E. Snowden and P. R. Unwin, in *Annual Review of Analytical Chemistry, Vol 6*, eds. R. G. Cooks and J. E. Pemberton, Annual Reviews, Palo Alto, 2013, vol. 6, pp. 329-351.
310. M. Wasberg and G. Horanyi, *Journal of Electroanalytical Chemistry*, 1995, **385**, 63-70.
311. C. Almeida, B. F. Giannetti and T. Rabockai, *Journal of Electroanalytical Chemistry*, 1997, **422**, 185-189.
312. B. H. Gu, W. J. Dong, G. M. Brown and D. R. Cole, *Environmental Science & Technology*, 2003, **37**, 2291-2295.
313. K. D. Hurley and J. R. Shapley, *Environ. Sci. Technol.*, 2007, **41**, 2044-2049.
314. K. D. Hurley, Y. X. Zhang and J. R. Shapley, *Journal of the American Chemical Society*, 2009, **131**, 14172.
315. A. Cano, P. Canizares, C. Barrera, C. Saez and M. A. Rodrigo, *Electrochemistry Communications*, 2011, **13**, 1268-1270.